Physical–Chemical Behavior of Dietary and Biliary Lipids during Intestinal Digestion and Absorption. 2. Phase Analysis and Aggregation States of Luminal Lipids during Duodenal Fat Digestion in Healthy Adult Human Beings†

Olle Hernell,‡ Joan E. Staggers,§ and Martin C. Carey*

Department of Medicine and Harvard Digestive Disease Center, Harvard Medical School, Gastroenterology Division, Brigham and Women's Hospital, Boston, Massachusetts 02115

Received March 6, 1989; Revised Manuscript Received September 19, 1989

ABSTRACT: Following the feeding of a triacylglycerol-rich meal to healthy adult human beings, duodenal contents were aspirated for ex vivo chemical and physical–chemical analyses. The aspirates were collected during established lipid digestion and absorption into a "cocktail" of chemical inhibitors that rapidly inhibited ex vivo lipolysis. Following ultracentrifugation, the lipids separated into a floating oil layer, several interfacial layers, a "clear" or turbid "subphase", and a precipitated "pellet". By chemical and phase analyses, the floating layer was composed of oil-in-water emulsion particles with cores of triacylglycerol (TG),[1] diacylglycerols (DG), and cholesteryl esters (CE) emulsified with a surface coat of partially ionized fatty acids (FA), monoacylglycerols (MG), diacylphosphatidylcholine (PL), and bile salts (BS). The interfacial layers contained similar emulsion particles dispersed among excess emulsifier which adopted a lamellar liquid-crystalline structure. Precipitated pellets were composed principally of emulsifying lipids, with smaller amounts of crystalline calcium soaps and BS. Relative lipid compositions of all but three subphases fell within a two-phase region of the condensed ternary phase diagram (Staggers et al., 1990, companion paper) where saturated mixed micelles composed of BS, FA "acid-soaps", MG, PL, cholesterol (Ch), and traces of DG (and TG) coexisted with unilamellar liquid-crystalline vesicles composed of the same lipids. Attempts to achieve clean separation of vesicles from micelles by repeat ultracentrifugation failed.[2] Compared with the structure and sizes of lipid particles in equilibrated model systems (Staggers et al., 1990), quasielastic light scattering (QLS) analysis revealed that ex vivo micellar sizes (mean hydrodynamic radii, $\bar{R}_h$) were similar (≤40 Å), whereas unilamellar vesicle sizes ($\bar{R}_h$ = 200–600 Å) were appreciably smaller. Two-component QLS analysis of the subphases showed that much larger proportions of lipids were solubilized by micelles than were dispersed as unilamellar vesicles. When followed as functions of time, vesicles frequently dissolved spontaneously into mixed micelles, indicating that, in the nonequilibrium in vivo conditions, the constituent micellar phase was often unsaturated with lipids. These results are consistent with the hypothesis that, during hydrolysis of emulsified DG and TG by luminal lipases, unilamellar vesicles originate in lamellar liquid crystals that form at emulsion–water interfaces in the upper small intestine. In a BS-replete environment, unilamellar vesicles probably represent the primary dispersed product phase of human fat digestion and facilitate the dissolution of lipolytic products into unsaturated mixed micelles. We speculate that saturation of mixed micelles by unilamellar vesicles produces the most favorable thermodynamic condition for maximizing lipid absorption rates from the upper small intestine; further, lipolytic products dispersed as uni- and multilamellar vesicles may explain the slow, but efficient, fat absorption that takes place from the entire small intestine in BS-deficiency states.

More than 95% of the 100–150 g of lipid consumed daily by an average Western adult is long-chain triacylglycerol (TG).[1] Before absorption into enterocytes, each TG molecule must be hydrolyzed into its absorbable products, two partially ionized fatty acid (FA) and one *sn*-2 monoacylglycerol (MG). In healthy human adults, this enzymatic hydrolysis is catalyzed sequentially by gastric lipase secreted by the chief cells of the stomach (Moreau et al., 1988) and by colipase-dependent pancreatic lipase secreted into duodenal contents by the pancreas (Borgström, 1977; Patton, 1981; Carey, 1983a; Carey et al., 1983; Hernell et al., 1988). Other lipid components of the diet, as well as the diacylphosphatidylcholine (PL) of bile,

† Supported in part by Research Grant DK 36588 and Center Grant DK 34854 (M.C.C.), NRSA Fellowship AM 07512 and Institutional Training Grant AM 07121 (J.E.S.), and Fogarty International Fellowship TW 03521 (O.H.), all from the National Institutes of Health, U.S. Public Health Service. O.H. received grants-in-aid from the Swedish Medical Research Council, the Sweden–America Foundation, the Henning and Johan Throne Holst Foundation, and Pfrimmer/Meda AB (Sweden).

* Correspondence should be addressed to this author at the Department of Medicine, Brigham and Women's Hospital, 75 Francis Street, Boston, MA 02115.

‡ Present address: Department of Pediatrics, University of Umeå, S-90185 Umeå, Sweden.

§ Present address: Merck, Sharp and Dohme Research Laboratories, Blue Bell, PA 19422.

[1] Abbreviations: QLS, quasielastic light scattering; $\bar{R}_h$, mean hydrodynamic radius; R_h, hydrodynamic radius; BS, bile salt; FA, fatty acid; TG, triacylglycerol; DG, diacylglycerol; MG, monoacylglycerol; PL, diacylphosphatidylcholine; Ch, cholesterol monohydrate; CE, cholesteryl ester; cmc, critical micellar concentration; imc, intermicellar concentration.

[2] On the basis of the present data and phase analyses of lipid compositions in the literature, we demonstrate subsequently that, by employing even the most severe ultracentrifugation techniques, micelles and unilamellar vesicles cannot be "cleanly" separated in the "subphases" of ex vivo duodenal fluid. This contrasts with the relative ease with which this was achieved in model systems of pure lipids patterned after aqueous duodenal contents (Staggers et al., 1990).

0006-2960/90/0429-2041$02.50/0

must also be hydrolyzed into more polar absorbable products; in particular, pancreatic phospholipase A_2 hydrolyzes a variety of PL molecules into lysophospholipids and FA (DeHaas et al., 1968; Verheij et al., 1980), and pancreatic carboxyl ester hydrolase hydrolyzes the ester linkages of a variety of dietary lipids, i.e., steryl and lipovitamin esters as well as acylglycerols (Lombardo & Guy, 1980; Bläckberg et al., 1981; Hernell et al., 1988).

Although much work has been devoted to exploring the various biochemical steps in lipid digestion [reviewed in Borgström (1977), Patton (1981), Carey et al. (1983), Verger (1984), Borgström and Erlanson-Albertsson (1984), and Hernell et al. (1988)], much less attention has been paid to the physical–chemical events involved. According to the classic studies of Hofmann and Borgström (1962, 1964), dietary lipids distribute between two (or three) physical states in duodenal contents: an oily or emulsion portion, rich in TG and diacylglycerol (DG); a dilute, aqueous mixed micellar phase composed of bile salts (BS) and lipolytic products; and, frequently, a precipitated "pellet". Because aqueous solubilities of partially ionized long-chain FA and MG are extremely low (nanomolar to micromolar range) (Hofmann & Mekhjian, 1973; Small, 1986) but increase considerably in the presence of BS above their critical micellar concentrations (cMC) (Hofmann, 1963), mixed micelles have been considered the sole vehicles for solubilization and transport of lipolytic products from the emulsion surfaces to the enterocytes (Thomson & Dietschy, 1981). Furthermore, lipid uptake is believed to be monomeric, and therefore mixed micelles of BS and lipolytic products provide a favorable concentration gradient across unstirred layers and mucosal surfaces. Solubilization of lipolytic products within BS micelles has therefore been considered a rate-limiting step in absorption of dietary and biliary lipids. However, in the complete absence of intraluminal BS, 50–75% of dietary TG is absorbed (Porter et al., 1971), suggesting that nonmicellar mechanisms for dispersion of lipolytic products are of importance in assimilation of alimentary tract lipids.

Under conditions patterned after human duodenal contents [reviewed in Patton et al. (1985)], Patton and Carey (1979) "visualized" in vitro lipolysis microscopically and identified crystalline as well as liquid-crystalline phases. On the basis of preliminary studies (Stafford et al., 1981; Stafford & Carey, 1981), Carey and co-workers (Carey et al., 1983) and Borgström (1985) have suggested that the model of Hofmann and Borgström (1962, 1964) may be an oversimplification and that, in aqueous duodenal contents, a mixed micellar and a liposomal (liquid crystalline) phase may coexist during established fat digestion. In these earlier studies, both phases appeared to be saturated with lipolytic products, suggesting their possible importance for efficient intestinal absorption of dietary lipids (Carey, 1983a; Carey et al., 1983).

In the present work we have systematically explored the physical chemistry of fat digestion in healthy adult human beings. Employing lipase-inhibited postprandial aqueous duodenal contents, we have paid particular attention to the existence, characteristics, and origin of liquid-crystalline phases. Most notably, we have obtained direct evidence for the coexistence of small unilamellar vesicles and mixed BS micelles in the aqueous-rich portion of duodenal contents. On the basis of these results and reevaluation of literature data, we propose that unilamellar vesicles represent an early product "phase" of lipolysis and originate from multilamellar vesicles (liposomes) at the surfaces of emulsion particles. The subsequent fate of vesicles, and their principal role in healthy adult human beings, is probably that of supplying mixed lipid products, in a readily dissolvable form, to the micellar phase for further solubilization and absorption.

Materials and Methods

Duodenal Intubations. After providing written informed consent, four healthy adult males (30–40 years of age) volunteered, two once and two twice, for a total of six separate duodenal intubations. Following an overnight fast, a silicone Salem sump tube (o.d. 0.4 cm, length 122 cm; Argyle, St. Louis, MO) with six side ports located within 5 cm of the tip was swallowed *per os* and, under fluoroscopic control, was placed in the duodenum at the angle of Trietz.

Composition of the Test Meal. The meal consisted of 50 g of commercial olive oil, 1 raw egg, 20 g of sucrose, 5 mL of vanilla extract, and 250 mL of 0.15 M NaCl and was brought to a total volume of 400 mL with water. Prior to administration, the meal was vigorously mixed by shaking at 37 °C for 30 min. Each meal took generally 5 min to drink, and this time point was considered "zero time" for the start of an experiment. A few milliliters of the meal was retained for compositional analysis.[3]

Duodenal Aspirates: Inhibition of Lipolysis and Bacterial Growth. At various times, usually at 60 and 90 min following the meal, 10–15 mL samples of duodenal contents were collected by siphonage or by gentle suction with a syringe into test tubes containing methanolic solutions of a "cocktail" of lipase inhibitors and antimicrobial agents, whereafter the tubes were capped under N_2. The cocktail of lipase inhibitors was composed of 50 mM diisopropylfluorophosphate, 50 mM diethyl (*p*-nitrophenyl)phosphate, 50 mM acetophenone (all from Sigma Chemical Co., St. Louis, MO), and 250 mM phenylboronic acid (Aldrich, Milwaukee, WI). To prevent bacterial growth, 5 μL of an aqueous solution of 8% NaN_3 (w/v) and 10% chloramphenicol (w/v) per milliliter of aspirated duodenal contents was also added to each tube prior to sample collection. As discovered in preliminary experiments, these additives were absolutely necessary to prevent bacterial multiplication, since gross contamination seriously interfered with measurement of lipid particle sizes by quasielastic light scattering (QLS) (see below). The tubes were gently mixed at 37 °C and maintained on a heating block at this temperature until lipid extractions were performed. In no case did the total volume of inhibitor solutions represent more than 2% (by volume) of the collected luminal contents. Further, since we compared ex vivo systems with model systems (Staggers et al., 1990), the lipolysis inhibitors were shown in preliminary experiments to have no appreciable effect upon the phase equilibria and physical chemistry of in vitro systems.

Duodenal Aspirates: Quantitation of Lipolysis Inhibition. To study lipolysis inhibition, six duodenal aspirates were treated as follows: One sample of duodenal contents (usually collected between the samples at 60 and 90 min) was at once divided into three portions, and one was immediately extracted for quantitative lipid analysis (see Materials and Methods). The methanolic solution of chemical inhibitors was added to the second; and, to the third, the same volume of methanol without inhibitors was added as a control. The latter two tubes were then incubated in a shaking water bath at 37 °C for 7 h prior to lipid extractions. To evaluate the efficiency of lipolysis inhibition, lipid compositions of all three samples were compared.

[3] Assayed composition of one meal was TG (118 mM), DG (2 mM), Ch (5.4 mM), and FA plus PL (7.8 mM).

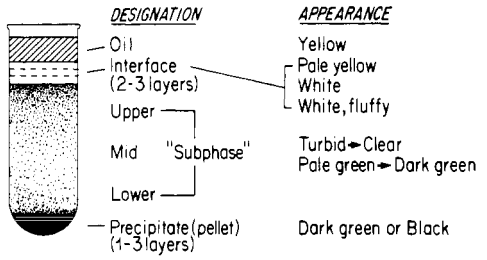

FIGURE 1: Schematic representation of a typical sample of distal duodenal contents following ultracentrifugation. Samples were ultracentrifuged as described under Materials and Methods and outlined in Table I. The duodenal contents were aspirated typically 60–90 min after a TG-rich meal, and enzymatic hydrolysis by pancreatic lipases was rapidly inhibited chemically (see Materials and Methods). From top to bottom of the centrifuge tube, the contents separated into an upper oil layer that grossly appeared yellow, one to several layers of interface that changed from pale yellow to fluffy white, a subphase that was optically clear or turbid, and a precipitate (pellet) that contained one to three dark layers. The actual sizes of individual layers varied widely between samples. The color of the subphase and pellet was variable but generally showed a gradation of pale green to dark green and black, due to oxidized bilirubin conjugates.

Separation and Collection of Phases in Duodenal Aspirates. Unless otherwise specified, all chemically inhibited aspirates were centrifuged at 37 000 rpm for 60 min (total centrifugal force, i.e., centrifugal force × time of centrifugation = 6×10^6 g·min) at 37 °C by using ultraclear tubes (13 × 51 mm) in a SW-50.1 swinging bucket rotor (Model L5-65 ultracentrifuge, Beckman Instruments, Palo Alto, CA). To minimize perturbation of the separated phases, the rotor was stopped without use of the centrifuge brake. In some experiments, ultracentrifugations were carried out in ultraclear tubes (11 × 34 mm) in a SW-55 swinging bucket rotor (Model TL-100 tabletop ultracentrifuge, Beckman Instruments) at 12000 rpm for 15 min (total centrifugal force, 1.5×10^5 g·min). Because centrifugal force times time determines, in part, the sedimentation distance of all particles, times of centrifugation were varied from 10 to 60 min to evaluate the effects of *total* centrifugal force upon phase separation. With other samples, as described below, the swinging bucket rotor was employed at 100000 rpm (246000*g*) for 5–8 h, yielding total centrifugal forces that varied from 6×10^7 to 1×10^8 g·min. The rotor was accelerated to 5000 rpm in 2 min (setting 4) and decelerated from 5000 rpm to a stop in 8 min (setting 8).

The separated layers (Figure 1) were aspirated from the centrifuged tubes in the following manner. After the side of a tube was penetrated with a 25-gauge needle, portions of the "subphase" were withdrawn by syringe, generally at the middle of the phase. Once a sufficient volume of subphase was obtained, the syringe was removed, and the needle was spigoted and left in place. A 50-μL Hamilton syringe (Hamilton Co., Reno, NV) was then used to penetrate the side of the tube at the level of the "interface". Only very small volumes (5–25 μL) of interfacial material could be withdrawn before this phase became visibly contaminated with overlying "oil" or by mixing with the subphase. Thereafter, when present in sufficient amounts, the oil portion was removed from the top of the tube by aspiration employing a disposable pipet or a 50-μL Hamilton syringe. Finally, the pelleted fraction was obtained by first removing all supernatant material from the tube and washing it with 0.15 M NaCl; this was followed by recentrifugation for 15 min at 25000rpm (6.2×10^5 g·min). The pellet was dispersed by vigorous vortex mixing in 0.1 mL of 0.15 M NaCl, and the mixture was then transferred by Pasteur pipet to a tared tube. In some experiments, aliquots of oil and/or interface were collected first to minimize their contamination by other layers. In particular, this procedure usually prevented further analysis of the subphases.

Chemical Analysis of Duodenal Aspirates and Separated Layers. Portions of total samples or separated phases from duodenal contents were subjected to total lipid extraction by a minor modification of the method of Folch and colleagues (Folch et al., 1957). To ensure complete protonation of FA, the organic solvent phases were partitioned with 0.2 volume of 0.15 M aqueous NaCl containing 2% glacial CH_3COOH [(v/v) pH ~3] and separated by centrifugation at 2000 rpm for 10 min (Staggers et al., 1982). The upper $MeOH/H_2O$ and lower $CHCl_3$ phases were aspirated into separate tubes and brought to known volumes with the same solvent and stored under a blanket of argon at −20 °C. Since BS partitioned into both phases, each was assayed for BS by using 3α-hydroxysteroid dehydrogenase (Sigma Chemical Co.) as described by Turley and Dietschy (1978). A physiologic mixture of purified taurine- and glycine-conjugated BS (Calbiochem-Behring, San Diego, CA) was employed as a standard [see Staggers et al. (1990)]. The $CHCl_3$ phase was found by densitometry (see below) to contain >95% of all other lipids. Total lipid concentrations were determined by triplicate dry weight measurements of the $CHCl_3$ phase. Total PL was measured by the organic PO_4 assay of Bartlett (1959). Protein was assayed by the method of Lowry (Lowry et al., 1951), using bovine serum albumin (Sigma Chemical Co.) as a standard. Total calcium was measured with the CALCM autoanalyzer pack (Du Pont Co., Wilmington, DE). All solvents were certified ACS spectroanalyzed grade obtained from Fisher Chemical Co. (Pittsburgh, PA). Reagent grade NaCl was roasted at 600 °C in a muffle furnace for 4 h to oxidize and remove organic impurities. H_2O was distilled in an all-glass Pyrex automatic still (Corning Glass Works, Corning, NY).

Separation and Densitometric Assays of Lipid Classes. Lipid standards used for thin-layer chromatographic separations [TG, DG, and MG, FA, cholesterol monohydrate (Ch), and cholesteryl oleate (CE)] were obtained from Nu-Chek Prep, Inc. (Elysian, MN), and were 99% pure as purchased. A solution of each standard was made in $CHCl_3$ at known concentration by dry weight determination, and mixtures (1 or 10 mg/mL of each lipid) were prepared by volume. All lipid solutions were stored in Teflon-lined screw-capped tubes under a blanket of argon at −20 °C. Aspirated luminal CE, Ch, FA, MG, DG, and TG were separated by thin-layer chromatography (Bitman et al., 1981) and measured by scanning thin-layer densitometry, essentially as described by Bitman and Wood (1981). Plates were prechanneled with a preadsorbent zone [Si 250-PA (19C), Baker Chemical Co., Phillipsburg, NJ)], and after a prewash in $(C_2H_5)_2O$, samples were applied by microliter capillary tubes (Drummond Scientific Co., Broomall, PA). Plates were developed first in $CHCl_3/CH_3OH/$glacial CH_3COOH (98:2:0.1 v/v/v) and, after drying under N_2 for 15 min, were redeveloped in $C_6H_{14}/(C_2H_5)_2O/$glacial CH_3COOH (94:6:0.2 v/v/v). For staining, plates were dipped for 3 s into a solution of 10% $CuSO_4$ (w/v) in 8% H_3PO_4 (v/v), whereafter spots were charred in a gas–liquid chromatograph oven (Shimadzu Model GC-9A, Columbia, MD) using a temperature program that increased from 50 to 180 °C at 10 °C/min. Within 1 h following charring, lipid classes were quantified by linear densitometry at 370 nm with a Shimadzu Model CS-930 dual-wavelength TLC scanner. Lipid masses in each spot were estimated from standard curves run simultaneously on each plate by employing eight different amounts of standards

(0.5–25 μg) for each lipid class. Within the concentration ranges studied, standard curves were linear ($r \geq 0.95$) and reproducible to within ±10%.

Quasielastic Light Scattering. Theory and application of QLS for the measurement of mean lipid particle (micelle and vesicle) sizes in aqueous solution have been described previously (Mazer et al., 1979). The instrumentation employed in the present study included a Spectra-Physics Model 164 argon ion laser (Spectra-Physics, Mountain View, CA) operating at a wavelength of 5145 Å, equipped with a Model 1096 Langley Ford autocorrelator (Langley Ford, Amherst, MA) interfaced to a Digital Equipment Corp. Professional 350 (Digital Equipment Corp., Marlboro, MA) computer with high data-storage capacity. Autocorrelation functions were fitted to one, two, or three components by a splicing function and analyzed as described (Cohen, 1986; Staggers et al., 1990). Particle number and lipid weight ratios in different particle populations were calculated from their respective sizes (hydrodynamic radius, R_h), fractions of scattered light, and appropriate form factors, assuming a bilayer thickness of 40 Å for unilamellar vesicles (Cohen, 1986; Staggers et al., 1990).

QLS of fractionated duodenal contents was carried out with samples in 6 × 50 mm glass tubes at a temperature of 37 ± 0.5 °C. When necessary, particularly with pure micellar samples, dust was sedimented by spinning for 10 min at 10000 rpm in a Model SS-4 Sorvall tabletop centrifuge (Du Pont). Measurements of mean hydrodynamic radius ($\bar{R}_h$) and polydispersity ($V\%$) were performed in triplicate on each sample, and the average values for each set of measurements are reported.

Freeze-Fracture Electron Microscopy. Small (1–4 μL) portions of separated subphases (Figure 1), sandwiched at 37 °C between two thin disks of >99% pure copper, were rapidly frozen in the liquid phase of partially solidified propane and were subsequently stored in liquid N_2. Specimens were then fractured in a Balzers 300 freeze-etch apparatus (Balzers, Hopewell Junction, NY) at a stage temperature of −105 °C by using a double-replica attachment as previously described (Madara, 1983). Specimens were then replicated with platinum–carbon at 45 °C, and to remove remaining tissue, replicas were cleaned in 3 M HNO_3 and sequentially washed in 25%, 50%, and 100% NaClO. Replicas were then washed in and floated on H_2O, picked up on formvar-coated 200-mesh hexagonal grids, and examined and photographed with a Philips 300 electron microscope (Philips Electronic Instruments, Mahwah, NJ).

Results

Collection and Centrifugation of Duodenal Contents. Table I displays the conditions of duodenal sample collection (15 samples) and centrifugation for the six intubation studies. In general, collection times were chosen at 60 and 90 min following ingestion of the meal since, in preliminary studies, the bulk of the meal passed through the duodenum during this interval. In some cases, collections at 75 and 120 min were carried out. Except for two collections from the midduodenum at 60 min, the middle of the collecting ports was verified to be at the angle of Trietz through each aspiration. As determined by measurement with a standard glass pH electrode (Radiometer Co., Copenhagen, Denmark), the pH of the separated subphases ranged from 6.1 to 8.1 (Table I). Identification of samples by the subjects' initials, times of collection, total centrifugal force, and centrifugation products are in some cases used in the text to highlight specific results. The designations of fractionated samples into oils, interfaces, subphases, and precipitates (pellets) are arbitrary distinctions that follow literature usage (Carey, 1983a). When used here, we imply that all the respective centrifugal fractions, including the so-called subphase,[2] were not true homogeneous phases. In fact, in all fractions where clean separation was achieved and which were suitable for further analyses (Table I), we show below that, with rare exceptions, none constituted a single phase within the rubric of the phase rule (Carey, 1983b). Due to collection difficulties as described under Materials and Methods, all collected fractions were not necessarily analyzed further, as will be evident from the tabulated data.

Inhibition of Lipolysis. In preliminary experiments with model systems, we found that no single inhibitor was completely effective in inhibiting colipase-dependent pancreatic lipase; hence, we employed a combination of diethyl (*p*-nitrophenyl)phosphate (Maylie et al., 1972) and phenylboronic acid (Gardner, 1980) to inhibit this lipase (Table II), diisopropyl fluorophosphate to inhibit carboxyl ester hydrolase (cholesteryl esterase) (Lombardo, 1982), and acetophenone to inhibit pancreatic phospholipase A_2 (Verheij et al., 1980).[4]

As shown by mean ± SD values in Table II, the cocktail of chemical inhibitors was very efficient in limiting hydrolysis. The FA concentration in samples with chemical inhibitors was 115 ± 10% (SD) compared with the immediately extracted samples, indicating an inhibitory efficiency of 87 ± 8%. On the basis of TG levels, the chemical inhibitory efficiency was 97 ± 38%. The large standard deviation in this case was due to two samples: one where inhibition of TG hydrolysis was only 62% (85%, on the basis of FA) and one in which there was a paradoxically higher TG concentration (169%) with inhibitors (128%, on the basis of FA). Because of extremely rapid hydrolysis by colipase-dependent pancreatic lipase (Borgström, 1977), it is likely that lipolysis in some aspirates took place either during aspiration or following collection, i.e., in the few moments prior to formation of an enzyme–inhibitor complex. However, it is also known that, under appropriate duodenal conditions, this lipase can synthesize TG from FA and MG (Patton, 1981; Hernell & Bläckberg, 1982). In the case of the aspirates without inhibitors (Table II), a considerable depletion in TG and DG occurred with corresponding elevations in FA. It is also noteworthy that an appreciable synthesis of CE took place.

Lipid Analysis of Total and Fractionated Postprandial Duodenal Contents. Table III lists all lipid compositions of unfractionated (and chemically inhibited) duodenal contents from each subject. Total lipid concentrations varied considerably between samples, from 31 to 233 mM (1.3–15.5 g/dL), with marked intersubject variation and a trend in most to be lower at the later sampling times. In particular, there was a pronounced variation in the size of the floating oil portion (Figure 1), which varied from a trace to almost 20% of the total volume with no consistent variation between subjects, sampling levels, or times of collection.

Table IV lists the absolute as well as relative lipid compositions of the fractionated oil layers (Figure 1) where some were visibly pure yellow oil (marked with an asterisk) but most were contaminated with white interfaces. The major constituents of the oil fractions were TG, DG, and FA. However, in these fractions, MG, PL, and BS were invariably present

[4] At the time these studies were performed, there was no known efficient inhibitor of gastric lipase [see Gargouri et al. (1988)]; however, this enzyme should have had little influence on the chemical species or physical-chemical states of duodenal lipids, since it is inhibited, in part, by BS above their cmc values and by partially ionized FA, it is readily digested by pancreatic proteolytic enzymes, and duodenal pH is unfavorable for its activity (Bernbäck et al., 1987, 1989).

Table I: Sampling of Duodenal Contents, Centrifugation Conditions, and Layers Analyzed[a]

no.	subject[b]	collection[c] (min)	sampling port	pH	centrifugation (g·min)	layers analyzed	recentrifugation (g·min)	layers analyzed
1	OH_1	60	Trietz	6.7	6×10^6	oil + interface		
						subphase	8×10^7	upper
								lower
		90	Trietz	6.5	6×10^6	oil + interface		
						subphase	1×10^8	upper
								lower
2	PG	60	Trietz	6.7	6×10^6	oil		
						interface		
						subphase	6×10^7	upper
								lower
		90	Trietz	6.4	6×10^6	oil		
						subphase	6×10^7	upper
								lower
		120	Trietz	6.2	6×10^6	subphase		
3	CP_1	60	Trietz	7.7	6×10^6	oil		
						interface + oil		
						subphase		
		75	Trietz	6.1	1.5×10^5	interface		
						subphase		
		75	Trietz	6.1	3.0×10^5	subphase		
		90	Trietz	6.1	6×10^6	oil		
						interface		
						subphase		
4	MA	60	Trietz	7.7	6×10^6	oil		
						interface + oil		
						subphase	6×10^7	upper
								mid
								lower
							1.5×10^5	oil
								subphase
		90	Trietz	8.1	6×10^6	oil		
						interface + oil		
						subphase	6×10^7	upper
								mid
								lower
							1.5×10^5	oil
								subphase
5	OH_2	60	midduodenum	7.2	6×10^6	interface + oil		
						subphase		
						pellet		
					1.5×10^5	interface + oil		
						subphase		
		90	Trietz	7.3	6×10^6	interface + oil		
						subphase		
					1.5×10^5	interface + oil		
						subphase		
6	CP_2	60	midduodenum	7.4	6×10^6	pellet		
		90	Trietz	6.5	6×10^6	pellet		
					1.5×10^5	pellet		

[a] Exact collection and centrifugation conditions are described under Materials and Methods. [b] Subjects' initials are used to designate specific samples discussed in text. [c] Collection time refers to time following administration of meal.

Table II: Inhibition of Lipolysis in ex Vivo Duodenal Contents[a] (n = 6)

lipid class[b]	with inhibitors[c]	without inhibitors[c]
TG	96.6 ± 38.0	23.7 ± 22.4
DG	88.1 ± 40.0	70.1 ± 99.4
MG	111.4 ± 22.5	111.3 ± 159.4
FA	115.4 ± 10.2	295.8 ± 192.0
Ch	88.6 ± 22.8	75.0 ± 25.8
CE	93.0 ± 15.9	150.1 ± 77.8
PL	109.3 ± 17.3	90.9 ± 4.3
mean ± SD	100.3 ± 11.4	

[a] Values are expressed as a percent (mean ± SD) of each lipid class in duodenal aspirates that were immediately extracted with $CHCl_3$/CH_3OH (2:1 v/v). [b] Lipid abbreviations are listed in footnote 1. [c] One portion of a sample of duodenal contents collected at each of the 6 intubations (between 60 and 90 min following a meal) was immediately extracted with $CHCl_3$/MeOH; two other portions were incubated in a shaking water bath for 7 h at 37 °C with added lipase inhibitors (see Materials and Methods) or with methanol as a control. Following extraction with $CHCl_3$/MeOH, lipid classes were separated and quantified as described under Materials and Methods.

except in one subject (PG), who showed no BS in this portion. The relative lipid compositions are grouped into (A) insoluble amphiphile (Ch), (B) insoluble oily amphiphiles (TG, DG, CE), and (C) swelling plus soluble amphiphiles (FA as "acid soap", MG, PL, and BS) for subsequent phase analysis. As shown by the high mean values of the visibly purest oils (n = 6), these contained an average of 1.4 M total lipid, of which 67% was TG/DG/CE (Table IV).

Table V displays all absolute and relative lipid compositions of interfacial fractions, although some (not marked with an asterisk, Table V) were contaminated with visibly yellow oil. Compared to the floating oil portions (Table IV), the interfaces were enriched in the more polar lipids, FA, MG, PL, and BS, particularly when normalized for the same concentration of oily amphiphiles (TG, DG, CE). The relative lipid compositions (A–C) are grouped as in Table IV for subsequent phase analysis. As shown by mean absolute and relative lipid compositions (n = 3), in "pure" interfaces (no visible oils), the samples were considerably enriched with swelling amphiphiles

Table III: Unfractionated Lipid Compositions of Luminal Contents

	time (min)	Ch (mM)	FA (mM)	MG (mM)	DG (mM)	TG (mM)	PL (mM)	BS (mM)	CE (mM)	total (mM)
OH_1	60	0.9	9.9	2.6	5.0	13.7	4.3	18.7	0.1	55.2
	90	1.0	6.5	1.3	1.8	2.6	4.2	13.6	0.1	31.1
PG	60	3.7	41.6	17.5	10.6	43.3	4.3	8.5	nd[a]	129.5
	90	1.9	40.7	4.7	22.0	151.9	5.7	5.8	0.2	232.9
	120	1.7	12.3	2.9	2.9	14.4	5.2	8.7	nd	48.1
CP_1	60	2.5	11.5	5.1	0.5	0.5	9.4	37.0	nd	66.5
	90	1.8	15.7	3.7	9.1	19.8	4.7	7.5	nd	62.3
MA	60	7.7	41.1	7.4	13.7	77.0	4.3	17.8	1.2	170.2
	90	2.1	19.5	3.6	4.5	10.9	4.4	15.9	nd	60.9
OH_2	60	0.8	6.8	2.8	2.7	28.5	2.3	9.0	0.3	53.2
	90	2.0	18.7	7.7	7.1	17.9	3.7	16.5	0.3	73.9
	mean ± SD	2.4 ± 2.0	20.4 ± 14.0	5.4 ± 4.5	7.3 ± 6.3	34.6 ± 44.5	4.8 ± 1.8	14.5 ± 8.8	0.2 ± 0.4	89.4 ± 62.2

[a] nd = not detected.

Table IV: Lipid Compositions of Oils ± Contaminating Interfaces

	time (min)	A Ch (mM)	B TG (mM)	B DG (mM)	B CE (mM)	C FA (mM)	C MG (mM)	C PL (mM)	C BS (mM)	total (mM)	mol/100 mol A	mol/100 mol B	mol/100 mol C
OH_1	60	10.3	159.3	40.3	1.2	91.9	19.6	8.9	19.1	350.6	2.9	57.3	39.8
	90	4.6	21.3	27.9	1.1	59.5	4.0	6.0	14.8	139.2	3.3	36.1	60.6
PG	60*	15.5	1301.3	227.1	nd[a]	626.6	113.0	nd	nd	2283.5	0.7	66.9	32.4
	90*	9.4	1460.0	190.3	8.0	525.8	203.4	18.5	nd	2415.4	0.4	68.7	31.0
CP	60*	9.2	282.0	94.0	36.8	210.6	26.2	9.8	13.2	681.8	1.4	60.6	38.1
	75	8.0	90.7	58.8	0.9	100.0	21.4	37.9	10.3	328.0	2.4	45.9	51.7
	90*	63.6	535.4	135.0	57.8	277.7	22.7	15.3	7.7	1115.2	5.7	65.3	29.0
MA	60*	43.9	641.8	126.4	2.1	349.1	91.0	8.8	7.9	1271.0	3.5	60.6	35.9
	90*	30.0	583.8	94.5	nd	235.7	22.5	6.8	10.1	983.4	3.1	69.0	28.0
	mean[b]	29 ± 22	801 ± 468	145 ± 54	18 ± 24	371 ± 169	80 ± 72	9.9 ± 6.5	6.5 ± 5.4	1458 ± 718	2.5 ± 2.0	65.2 ± 3.8	32.4 ± 3.9

[a] nd = not detected. [b] Mean ± SD of "pure" oils (n = 6, starred).

Table V: Lipid Compositions of Interfaces ± Contaminating Oils

	time (min)	A Ch (mM)	B TG (mM)	B DG (mM)	B CE (mM)	C FA (mM)	C MG (mM)	C PL (mM)	C BS (mM)	total (mM)	mol/100 mol A	mol/100 mol B	mol/100 mol C
PG*	60	1.9	84.8	28.1	nd[a]	57.2	10.5	4.4	11.1	198.0	1.0	57.0	42.0
CP	60	7.6	169.5	59.6	26.1	278.3	18.3	9.9	45.8	615.1	1.2	41.5	57.3
CP*	75	5.3	45.3	31.0	1.0	59.4	16.0	8.7	13.0	179.7	3.0	43.0	54.0
CP*	90	15.6	367.9	14.2	7.9	284.5	32.2	15.8	6.3	744.4	2.1	52.4	45.5
MA	60	5.5	62.4	21.8	0.2	57.8	5.1	4.2	17.2	174.2	3.2	48.5	48.4
MA	90	16.1	141.5	40.3	nd	65.8	15.8	5.0	9.6	294.1	5.5	61.8	32.7
OH_2	60	1.8	244.1	19.3	1.2	32.9	16.5	4.2	12.3	332.3	0.5	79.6	19.8
OH_2	90	3.1	110.8	42.3	1.4	87.7	21.7	5.3	16.5	288.8	1.1	53.5	45.4
OH_2	60	1.8	128.4	16.1	0.7	30.4	5.6	4.3	10.2	197.5	0.9	73.5	25.6
OH_2	90	3.2	88.0	43.7	1.2	74.1	28.8	5.2	19.6	263.8	1.2	50.4	48.4
	mean[b]	7.6 ± 7.1	166 ± 176	24.4 ± 9	3.0 ± 4.3	134 ± 131	19.6 ± 11.3	9.6 ± 5.8	10.1 ± 3.5	374 ± 321	2.0 ± 1.0	50.8 ± 7.1	47.2 ± 6.2

[a] nd = not detected. [b] Mean ± SD of purest interfaces (n = 3, starred).

(component C, 47%, Table V, compared with 31% for purest oils in Table IV). The mean total lipid concentration of the purest interfaces was 0.37 M, or 26% of that in the oil layer.

The absolute and relative lipid compositions of all total subphases as well as those further fractionated after repeat ultracentrifugation (see Materials and Methods) are listed in Table VI. These fractions were strikingly more dilute than the oils or interfaces (range 3.7–97.5 mM, mean 2.94 ± 19.7 mM, or approximately 1.3 g/dL), the mean lipid concentration being 33% of the unfractionated samples (Table III). The subphases were enriched mostly in FA, MG, PL, and BS, with only traces (or no) DG, TG, and CE. BS concentrations ranged from 1.8 mM [below the intermicellar concentration (imc) of mixed BS at the micellar phase limit; see Staggers et al. (1990)] to 65 mM (mean 13.1 ± 11 mM), and in those fractions subjected to a second ultracentifugation (marked upper, middle, and lower, Table I), a BS as well as an FA and MG concentration gradient was created down the centrifuge tubes (Table VI). The mean FA:MG ratio was 3:1 but varied, from a theoretical 2:1 for TG hydrolysis by pancreatic co-lipase-dependent lipase alone (Borgström, 1977) to a high level of 15:1. The relative lipid compositions and phase analyses of these systems are described below.

Table VII lists the absolute and relative lipid compositions of the precipitated pellets. While all lipid classes were identified in the pellets, the greatest enrichment was in FA, MG, and PL; phase analyses of these compositions are presented below. The pelleted volume varied among samples, but always represented only a few percent (<5%) of total volume. The calcium concentration averaged 12.5 ± 12.5 μmol/g, compared with 87 ± 37 μmol/g for FA (n = 4). Hence, it is likely that only ~15% of FFA precipitated in the form of calcium soaps. Mean (±SD) protein content of the pelleted fractions was 9.8 ± 1.0 mg/g (n = 4).

Phase Analysis of Oils, Interfaces, and Precipitates. Figure 2 displays the o/w emulsion phase diagram of Miller and Small (1982, 1983) on which we have plotted the relative lipid compositions of the oils, interfaces, and precipitated pellets. This truncated phase diagram (with total lipid fixed at 40 g/dL) shows percent Ch on the left axis, percent FA/MG/PL

Table VI: Lipid Compositions of Subphases

	time (min)		A Ch (mM)	B FA (mM)	B MG (mM)	B DG (mM)	B TG (mM)	B PL (mM)	C CE (mM)	C BS (mM)	total (mM)	mol/100 mol A	mol/100 mol B	mol/100 mol C
OH_1	60	total	0.4	3.2	0.7	tr[a]	tr	4.1	nd	14.8	23.2	1.7	34.5	63.8
	60	upper	nd[b]	0.6	0.1	nd	nd	0.6	nd	6.3	7.6	0	17.1	82.9
	60	lower	0.3	2.4	0.4	nd	nd	2.6	nd	14.9	20.6	1.5	26.2	72.3
	90	total	0.6	1.6	0.4	0.2	tr	4.2	nd	11.2	18.2	3.3	35.2	61.5
	90	upper	0.3	2.4	0.5	nd	nd	2.0	nd	8.3	13.5	2.2	36.3	61.5
	90	lower	0.5	4.3	0.9	nd	nd	4.3	nd	15.0	25.0	2.0	38.0	60.0
PG	60	upper	0.5	7.5	1.9	nd	0.1	2.3	nd	7.3	19.7	2.7	60.1	37.1
	60	lower	0.6	7.9	2.1	nd	0.2	2.5	nd	8.3	21.6	2.8	58.8	38.4
	90	total	0.3	2.8	1.0	0.2	nd	1.3	nd	6.4	12.0	2.5	44.2	53.3
	90	upper	0.3	6.0	0.7	0.1	nd	1.9	nd	5.6	14.6	2.1	59.2	38.4
	90	lower	0.3	3.2	0.5	nd	nd	1.9	nd	7.6	13.5	2.0	41.5	56.3
	120	total	0.4	4.3	2.4	0.2	0.1	13.3	nd	7.9	28.7	1.4	70.9	27.5
CP_1	60	total	2.1	17.8	5.2	nd	nd	7.3	nd	65.1	97.5	2.2	31.1	66.8
	75	total	1.5	25.6	8.6	0.2	0.4	6.4	nd	18.2	60.9	2.5	67.7	29.9
	75	total	1.4	23.2	8.1	0.2	0.4	1.7	nd	20.3	55.3	2.5	60.8	36.7
	90	total	0.6	4.4	0.3	0.1	nd	4.0	nd	12.5	21.9	2.7	40.3	57.1
MA	60	total	1.4	16.3	10.9	0.5	0.2	3.5	0.1	13.7	46.6	3.0	67.6	29.4
	60	upper	0.5	6.4	0.8	nd	nd	1.6	nd	6.4	15.7	3.2	56.1	40.8
		mid	0.6	13.5	2.2	nd	nd	2.8	nd	12.4	31.5	1.9	58.7	39.4
		lower	1.9	25.1	3.7	0.1	0.3	3.2	0.1	13.9	48.3	3.9	67.3	28.8
	60	total	1.2	18.1	7.4	0.6	nd	3.6	nd	11.6	42.5	2.8	69.9	27.3
	90	total	1.5	14.9	6.7	0.2	0.1	3.6	nd	16.0	43.0	3.5	59.3	37.2
	90	total	1.3	14.6	4.2	0.3	nd	3.6	nd	19.7	43.7	3.0	51.9	45.1
	90	upper	0.1	3.3	0.8	nd	nd	1.3	nd	5.4	10.9	0.9	49.5	49.5
		mid	0.9	11.0	1.7	0.4	nd	3.0	nd	13.5	30.5	3.0	52.8	44.3
		lower	0.9	11.6	1.5	0.3	nd	0.6	nd	14.5	29.4	3.1	47.6	49.3
OH_2	60	total	0.1	0.8	0.3	nd	nd	0.7	nd	1.8	3.7	3.5	48.3	48.3
	60	total	0.4	2.8	0.9	0.1	nd	1.7	nd	2.6	8.5	4.7	64.7	30.6
	90	total	1.2	11.6	4.3	nd	nd	3.1	nd	17.0	37.2	3.2	51.1	45.7
	90	total	1.1	12.1	4.3	nd	nd	3.1	nd	15.3	35.9	3.1	54.3	42.6
	mean ± SD		0.77 ± 1.6	9.3 ± 7.4	2.8 ± 2.9	0.1 ● 0.2	0.06 ± 0.2	3.2 ± 2.5	0.01 ± 0.03	13.1 ± 10.8	29.4 ± 19.7	2.6 ± 0.9	50.7 ± 13.9	46.7 ± 14.4

[a] tr = trace. [b] nd = not detected.

Table VII: Lipid Compositions of Precipitates (Pellets)

	time (min)	A Ch (mM)	B TG (mM)	B DG (mM)	B CE (mM)	C FA (mM)	C MG (mM)	C PL (mM)	C BS (mM)	total (mM)	mol/100 mol A	mol/100 mol B	mol/100 mol C
OH_2	60	4.2	3.5	3.4	0.4	56.0	17.9	19.0	4.9	109.3	3.8	6.7	89.5
CP_2	60	1.9	3.8	3.2	nd[a]	139.2	4.5	3.0	2.2	157.7	1.2	4.4	94.4
	90	7.2	0.8	5.2	nd	64.2	16.2	4.6	5.7	103.9	6.9	5.8	87.3
	90[b]	4.4	1.0	9.5	nd	86.6	13.2	6.8	7.1	128.6	3.4	8.2	88.4
	mean ± SD	4.4 ± 2.2	2.3 ± 1.6	5.3 ± 2.9	0.1	86.5 ● 37.4	12.9 ± 6.0	8.3 ± 7.3	5.0 ± 2.1	124.9 ± 24.3	3.8 ± 2.4	6.3 ± 1.6	89.9 ± 3.1

[a] nd = not detected. [b] 1.5×10^5 g·min.

and BS[5] on the upper horizontal and right axes, and percent TG/DG/CE on the base axis. Along the left axis is a one-phase region containing essentially pure TG/DG/CE oil, graphed by a short thickened line parallel to this axis and extending upward from 0 to ~6% Ch. This phase can solubilize less than 1% FA/MG/PL/BS, and its length shows that it becomes saturated with ~6 mol % Ch. On the right side of the diagram is another one-phase region, composed of a lamellar liquid-crystalline phase of FA (partially ionized acid soap)/MG/PL and BS. While this phase can solubilize <4% TG/DG/CE, it can solubilize ~35 mol % Ch at equilibrium. Between these one-phase regions is a two-phase zone composed of variable proportions of the two phases at each side. The directions of the tie-lines are shown by the interrupted line connecting an open diamond, representing overall relative lipid composition, to solid diamonds, representing relative lipid composition of the two phases. As shown in the inset, stable emulsion particles are *two*-phase systems; the TG/DG/CE in the core is represented by the one-phase oil composition on the left, and the FA/MG/PL/BS emulsifying monolayer is shown by the one-phase liquid-crystalline composition on the right. Miller and Small (1982, 1983) showed that, as the overall composition of laboratory-made emulsion particles moved from left to right across this phase diagram, the sizes of the particles became progressively reduced as the proportion emulsifying to core lipids was increased. At about 60% core lipid, the emulsion particles attained their minimum sizes. With further decreases in the ratio of core lipids to emulsifying lipids, the latter were found in excess, separating from the emulsion particles as a coexisting lamellar liquid-crystalline phase. The plots of the relative lipid compositions of the oily layers (Table IV) from the present experiments show that the majority contained ≥60% core lipids and, by analogy with in vitro systems, were therefore macroemulsion particles reduced to their smallest permissible sizes.

In contrast, the interfacial layers generally contained ≤60% core lipids and therefore had excess emulsifying lipid present as lamellar liquid crystals. The presence of liquid crystals was verified experimentally in many of these fractions employing polarizing microscopy and displayed a focal conic (Maltese

[5] Although bile salts are soluble amphiphiles (Small, 1971) and not emulsifiers per se, they promote the emulsifying potential of intestinal swelling amphiphiles (partially ionized FA/MG/PL) (Carey, 1983a). Although not included in the phase diagram of stable emulsions by Miller and Small (1982, 1983), it is appropriate to include BS in this phase analysis, since the proportions present (Tables IV and V) should not alter appreciably the liquid-crystalline structures or the phase relations (Small, 1971).

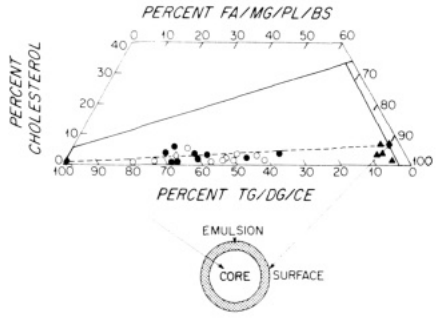

FIGURE 2: Relative lipid compositions of oils, interfaces, and precipitates (pellets) of separated duodenal contents. In this truncated ternary phase diagram (Miller & Small, 1982; Carey et al., 1983), the more polar lipids (FA, MG, PL, and BS) were grouped as one component, the less polar lipids (CE, TG, and DG) was grouped as a second component, and Ch was the third component. By visual inspection, predominant oils and predominant interfaces were, in many cases, contaminated with each other during collection. The precipitates (pellets) were analyzed from duodenal aspirates of two subjects (OH_2 and CP_2) at 60 and 90 min (Table VII). The phase diagram shows that, when mixed in all proportions, the equilibrium physical state of the more polar lipids is a one-phase lamellar liquid-crystalline zone that can solubilize ~35% Ch and only ~3% of the less polar (oily) lipids. The latter form a small one-phase oil zone capable of solubilizing 6% Ch and only traces of the more polar lipids. All compositions plotting between these two-phase zones are composed of two phases. As shown by the typical tie-line, the phase composition of a system shown (open diamond) is composed of two phases with compositions subtended to the ends of the tie-lines and falling on the boundary of the one-phase regions (solid diamonds). As shown in the inset, a stable intestinal emulsion has core lipids composed of TG, DG, and CE and emulsifying lipids composed of FA/MG/PL/BS. The oily portions of centrifuged intestinal contents (solid symbols) were more rich in core lipids than the interfaces (open symbols), although overlap was considerable. The lipids of the precipitated pellets (triangles) plotted close to the limit of the liquid-crystalline phase and were predominantly lamellar liquid crystals with some calcium soaps. As discussed in the text, most interfaces were composed of the smallest permissible emulsion particles with excess emulsifier frequently present as a lamellar liquid-crystalline phase.

cross) texture. The precipitated (or pelleted) material was composed essentially of the emulsifying lipids. Besides the content of calcium soaps (~15%) and protein (~10%) in the precipitates, ~75% of the pelleted material was liquid-crystalline lipid and other crystalline and amorphous material, as verified by polarizing microscopy, but was not further separated or identified chemically.

Phase Analysis of Subphases. Figure 3 displays a series of truncated phase diagrams interpolated from data in the preceding paper (Staggers et al., 1990) designed for variations in physical–chemical conditions encountered in ex vivo aqueous-rich duodenal contents of healthy adult humans in the present experiments. In each, percent (mixed) BS is plotted on the base axis, percent Ch on the left axis, and percent mixed (intestinal) lipid (FA, MG, PL, DG) on the top and right axes, respectively. The one-phase micellar zone is shown at the bottom left of each diagram, with the right-hand phase boundary of the micellar phase (Staggers et al., 1990) appropriate to the total lipid concentration, pH, and FA:MG ratio obtained in the actual aqueous duodenal sample plotted (Tables I and VI). The phase boundary of the lamellar liquid-crystalline phase on the right is shown as invariant with the physical–chemical conditions of the aqueous intestinal contents. The plotted relative lipid compositions represent whole subphases following a single ultracentrifugation (large symbols) as well as upper, middle, and lower fractions of subphases after a second and even third ultracentrifugation (smaller symbols). These show a broad distribution, ranging from well within the micellar zone (OH_1, CP), lying near the

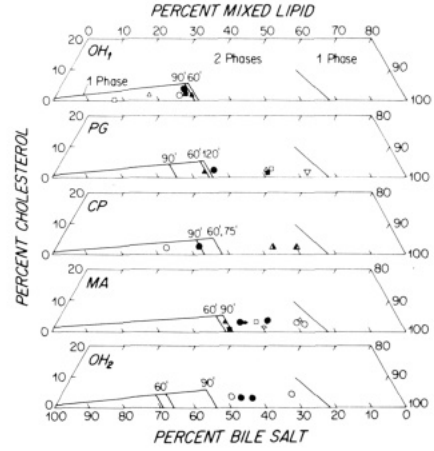

FIGURE 3: Relative lipid compositions of subphase fractions of duodenal contents, plotted on a series of truncated triangular phase diagrams [from Staggers et al. (1990)] with phase boundaries of the micellar phase appropriate to the pH, FA:MG ratio, and total lipid concentration of the samples (37 °C). Percent BS is plotted on the base axis, Ch on the left axis, and percent mixed lipid (principally FA, MG, and PL; see Table VI) on the upper and right axes. For each subject, open circles represent 60-min samples, solid circles 90-min samples, black and white triangles 75-min samples, and inverted triangles 120-min samples. Squares, diamonds, and triangles represent upper, middle, or lower fractions of the whole subphase at 60 (open symbols) and 90 (solid symbols) min (further discussed in text).

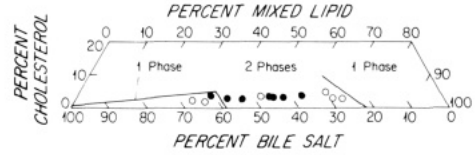

FIGURE 4: Relative lipid compositions of whole subphases separated from centrifuged duodenal contents aspirated from the angle of Trietz. Open and solid symbols represent duodenal fluid aspirated 60 and 90 min, respectively, following feeding a fatty meal to healthy human volunteers. The axes of the truncated triangular phase diagram are identical with those described in Figure 3. The phase boundary for the micellar phase was for typical physiological conditions (1 g/dL, pH 6.5, 37 °C, FA:MG ratio 5:1) (Staggers et al., 1990).

micellar phase boundary (OH_1, PG, CP), or spanning across the two-phase region (PG, CP, MA, OH_2) to almost reach the liquid-crystalline phase boundary. It is notable that the relative lipid composition of OH varied from micellar (OH_1) during the first study to the two-phase zone (OH_2) during the second intubation study (Figure 3). By phase analysis (Figure 4), the physical–chemical state of total aqueous subphase lipids of the postprandial duodenum was micellar in a few cases and therefore unsaturated with lipid; a few were micellar and saturated with lipid, whereas most were two-phase systems composed of saturated micelles and unilamellar vesicles that could not be separated ultracentrifugally (see below).

Physical Analysis of Subphases. Table VIII provides a list of overall $\bar{R}_h$ values by QLS in a subphase or fraction thereof and two-component R_h values by multicomponent QLS analysis and compares these results to the physical state of the subphases by phase analysis (as in Figure 3). In all cases, where the $\bar{R}_h$ values fell between 23 and 33 Å, the particle sizes were consistent with micelles, and the variances, an index of polydispersity (V values, Table VIII), were low, in excellent agreement with the values derived from model micellar systems ($\bar{R}_h$ values <40 Å, V values <30%) (Staggers et al., 1990). Further, in each case, when the $\bar{R}_h$ value indicated pure micelles, the relative compositions by phase analysis (Figure 3, Table VIII) indicated that the systems were indeed micellar without exception (Table VIII). This was not necessarily the

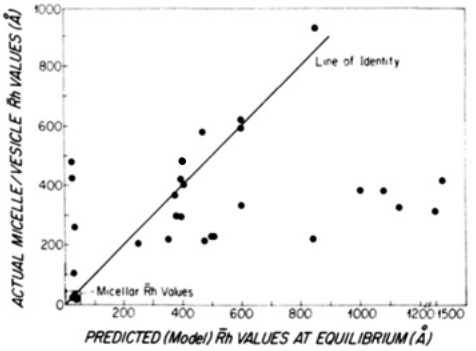

FIGURE 5: Comparison of actual particle sizes expressed as $\bar{R}_h$ values in the subphases of all duodenal contents with those predicted by the model systems (Staggers et al., 1990) for equivalent physical–chemical conditions of pH, total lipid concentration, FA:MG ratio, and lipid:BS ratios, but not *time*. An identity line is not obeyed, showing that native $\bar{R}_h$ values ($\bar{R}_h \sim 200$–600 Å), which principally represent vesicle sizes, were in general smaller than equilibrium sizes (5–7 days) of the vesicles in model systems.

case when $\bar{R}_h$ values indicated micelles plus vesicles ($\bar{R}_h > 100$ Å), since a few of these relative lipid compositions fell within the micellar zone (compare Figure 3 and Table VIII). Since the native systems were examined in the fresh state, the latter finding provides one line of evidence that native aqueous duodenal contents were in a nonequilibrium state and that a dynamic dissolution of vesicles by unsaturated micelles was taking place. Figure 5 provides further evidence of the metastability of lipids in aqueous duodenal content. Here, the actual micelle plus vesicle sizes (mean $\bar{R}_h$ values) are plotted versus the predicted sizes of equilibrated model systems appropriate to the pH, FA:MG ratio, and total lipid concentration of the aqueous duodenal content (Staggers et al., 1990). Figure 5 makes clear that, except for the tightly clustered set of micellar sizes, an identity relationship between the sizes of equilibrated vesicles in the model systems (examined at >7 days) and that in the native systems (examined at ~1–6 h) was not obeyed. With the exception of one outliner, all ex vivo $\bar{R}_h$ values fell between 200 and 600 Å (indicative of vesicle sizes), whereas the predicted vesicle sizes for the same experimental conditions at equilibrium extended to ~1500 Å. Figure 6 shows an electrophotomicrograph of a typical subphase with relative lipid composition falling well within the two-phase region. This reveals that liquid-crystalline vesicles are present solely as single bilayered structures (arrows) of small to medium size, closely approximating the sizes obtained by QLS (Figure 5). Neither the coexisting micelles nor putative nonbilayer phases were visualized.

Effect of Time and Centrifugal Force upon Subphase Particle Distribution. When postprandial duodenal contents were separated by different centrifugation conditions (Table I), there were generally no major differences in total lipid concentration or composition of the resulting subphases. The 1-h centrifugation at 100000*g* was chosen as a uniform condition for most of the samples so that direct comparisons could be made. However, we observed in some of the samples that conditions of centrifugation had a striking effect on the relative lipid and particle composition of the resulting subphases (Table VI and Figure 7). The greater the centrifugal force and/or time, the closer to the micellar phase boundary the subphase plotted, indicating a relative increase in micelle-to-vesicle ratios. Figure 7 displays relative lipid compositions following a second and third ultracentrifugation of the subphase. In two cases (Figure 7A), this procedure brought the relative compositions closer to the micellar phase boundary without true phase separation. This is particularly well illustrated by one sample

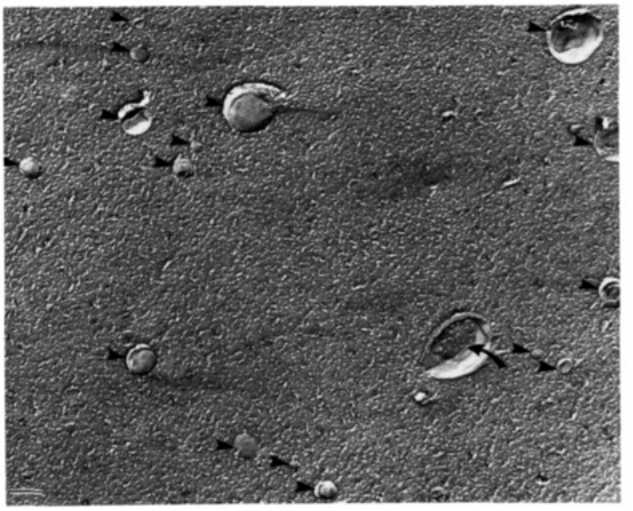

FIGURE 6: Freeze-fracture electron micrograph of aqueous-rich duodenal fluid. The sample was collected from the midduodenum, 60 min following a meal (OH_2), and centrifuged for 1.5×10^5 g·min, and the resulting subphase was kept for 1 h at 37 °C until frozen. The sample was collected and treated to obtain a subphase, free of oil and pellet constituents but maximally enriched in nonmicellar particles. Many unilamellar vesicle structures of heterogeneous size (shown by arrowheads) are present. The smooth surfaces of the vesicles represent fracture planes along the hydrophobic plane of a lipid bilayer. Cross-fractured vesicles (curved arrows) show that the vesicle interior is occupied by a solution with the same fracture-surface characteristics as the extravesicular solution. The bar in the lower left-hand corner represents 2000 Å.

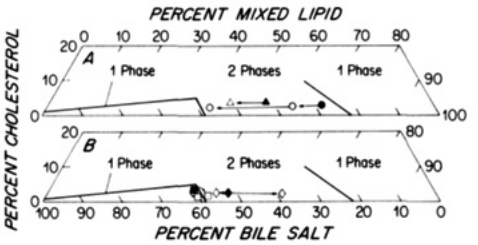

FIGURE 7: Relative lipid compositions of subfractions of "subphases" plotted on truncated triangular phase diagrams [phase boundaries from Staggers et al. (1990)]. (A) Triangular symbols represent subphases of OH_2 (90 min) that were centrifuged for 1.5×10^5 g·min (solid symbols) and 6×10^6 g·min (open symbols). Lower symbols (circles) represent subphases of CP_1 (90 min) that were centrifuged for 1.5×10^5 g·min (solid symbol), followed by 3.0×10^5 g·min (open symbol, middle) and 6×10^6 g·min (open symbol, left). (B) Solid symbols (diamonds and squares) represent relative lipid compositions of duodenal subphase of OH_1, 90 min (in two-phase region), and PG, 90 min (in micellar region), collected after centrifugation at 6×10^6 g·min. These were further centrifuted at 1×10^8 and 7×10^7 g·min, respectively, and the micellar and vesicle phases were collected from bottom and top of the subphase regions. For the relative lipid composition that fell within the micellar zone (squares), little change in relative composition occurred from top to bottom of subphase. In contrast, for the relative compositions that fell within the two-phase zone (diamonds), the individual phases were partially separated, allowing a tie-line to be drawn [cf. Staggers et al. (1990)].

(CP_1, 90 min) that was subjected to centrifugal forces 1.5×10^5, 3×10^5, and 6×10^6 g·min, respectively (Figure 7A, circles). At the highest centrifugal force the resultant subphase plotted very close to the micellar phase boundary with an $\bar{R}_h$ value of 31 ± 1 Å. The subphase obtained after the lowest centrifugal force produced an $\bar{R}_h$ value of 413 Å; the subphase from the intermediate ultracentrifugation produced an $\bar{R}_h$ value of 384 Å. The other sample (OH_2, 90 min, triangles) gave analogous results when total centrifugal forces of 1.5×10^5 and 6×10^6 g·min, respectively, were applied. QLS analysis in this case also showed a decrease in $\bar{R}_h$ values from 773 to

Table VIII: Physical States of Aqueous-Rich Subphases

subject	time (min)	sample	total (mM)	lipid (g/dL)	variance (%)	2-component R_h values (Å)	1-component[a] $\bar{R}_h$ values (Å)	physical state by phase analysis	physical state by $\bar{R}_h$ value
OH_1	60	total	23.2	1.2	502	na[b]	259	micelles (1ψ)[c]	micelles + vesicles (2ψ)[c]
		upper	7.6	0.4	45	na	471	micelles	micelles + vesicles
		lower	20.6	1.0	64	na	23	micelles	micelles
	90	total	18.2	1.0	293	na	102	micelles	micelles + vesicles
		upper	13.5	0.7	76	na	425	micelles + vesicles	micelles + vesicles
		lower	25.0	1.3	34	na	24	micelles	micelles
PG	60	total	na	na	59	na	340	na	micelles + vesicles
		upper	19.7	0.9	89	na	619	micelles + vesicles	micelles + vesicles
		lower	21.6	1.0	41	na	215	micelles + vesicles	micelles + vesicles
	90	total	11.9	0.6	32	na	294	micelles + vesicles	micelles + vesicles
		upper	14.5	0.5	57	na	576	micelles + vesicles	micelles + vesicles
		lower	13.4	0.7	53	41; 850	205	micelles + vesicles	micelles + vesicles
CP_1	60	total	97.5	4.6	62	na	33	micelles	micelles
	75	total	60.9	2.5	26	53; 772	413	micelles + vesicles	micelles + vesicles
	75	total	55.3	2.2	36	30; 730	384	micelles + vesicles	micelles + vesicles
	90	total	21.9	1.1	21	na	31	micelles	micelles
MA	60	total	46.6	1.9	37	89; 433	322	micelles + vesicles	micelles + vesicles
	60	total	42.5	1.7	39	na	308	micelles + vesicles	micelles + vesicles
	60	upper	15.7	0.7	45	84; 461	332	micelles + vesicles	micelles + vesicles
		mid	31.5	1.3	36	45; 288	222	micelles + vesicles	micelles + vesicles
		lower	48.3	1.9	34	102; 626	383	micelles + vesicles	micelles + vesicles
	90	total	43.0	1.8	49	29; 880	232	micelles + vesicles	micelles + vesicles
	90	total	43.7	1.9	18	na	296	micelles + vesicles	micelles + vesicles
	90	upper	10.9	0.5	31	78; 753	417	micelles + vesicles	micelles + vesicles
		mid	30.5	1.3	34	35; 502	365	micelles + vesicles	micelles + vesicles
		lower	29.4	1.2	30	12; 376	397	micelles + vesicles	micelles + vesicles
OH_2	60	total	3.7	0.2	29	na	482	micelles + vesicles	micelles + vesicles
	60	total	8.5	0.4	45	102; 1475	938	micelles + vesicles	micelles + vesicles
	90	total	37.2	1.6	62	23; 440	218	micelles + vesicles	micelles + vesicles
	90	total	35.9	1.6	37	29; 773	595	micelles + vesicles	micelles + vesicles

[a] 1-component refers to weighted mean hydrodynamic radius of all particle populations in the subphase. [b] na = not analyzed. [c] 1ψ and 2ψ denote one- and two-phase systems, respectively.

440 Å; however, when this sample was measured again after 3 h at 37 °C, its $\bar{R}_h$ value was 47 Å. In Figure 7B, two particle populations were partially separated from one subphase, allowing an incomplete tie-line to be drawn (PG, 90 min, diamonds). The $\bar{R}_h$ value of the overall composition was 262 ± 5.0 Å, which changed insignificantly to 236 ± 31 Å after 5 h at 37 °C. Following ultracentrifugation, the fraction that plotted near the micellar phase boundary gave an $\bar{R}_h$ value of 205 ± 26 Å. By two-component QLS analysis this sample was composed of mixed micelles (R_h = 41 Å) and vesicles (R_h = 850 Å). The separated fraction that plotted toward the liquid-crystalline phase limit gave an $\bar{R}_h$ value of 576 ± 37 Å, consistent with large vesicles. In the case of OH_1 at 90 min (Figure 7B, squares), the initial relative lipid composition of the subphase plotted within the micellar zone and had, at first, an $\bar{R}_h$ value of 102 ± 36 Å that fell to 27 ± 15 Å at 8 h (37 °C). Following 1.5×10^5 g·min centrifugation, the respective values for the upper and lower portions of the subphase also plotted in the vicinity of the micellar phase boundary. The earliest $\bar{R}_h$ value for one sample plotting inside the micellar zone was 425 Å; this also fell dramatically to 31 ± 44 Å at 15 min (37 °C). The relative lipid composition that plotted just outside the micellar zone gave a stable $\bar{R}_h$ value of 28 ± 3.1 Å. Thus, in all cases, not only did increased time and time plus centrifugation allow spontaneous dissolution of vesicles into micelles, but even the most rigorous ultracentrifugation conditions did not separate the two phases of the subphase, all attesting to the similar buoyant density of the two particles and possibly the low but perceptible production of vesicles by some continued lipolysis (see Table II).

In the present study, we also found exceptions to the general pattern: For example, with high *g* forces a BS/FA/MG gradient was created in the tube, with vesicles enriched on top of the subphase (Table VI). However, with some samples we also observed that particles of vesicle size were enriched both at the top *and* the bottom of the subphase. Two subphases, obtained after centrifugation for 6×10^6 g·min (MA 60 and MA 90), were subjected to a second centrifugation (6×10^7 g·min), whereafter fractions were collected from the top, middle, and bottom parts of the tubes. In the 60-min sample, the ratio of micelles to vesicles by two-component QLS analysis was highest in the middle of the tube, indicating vesicle enrichment at both the top and bottom. In contrast, the 90-min sample showed a continuous increase in both numerical and weight ratio of micelles to vesicles down the length of the tube (not illustrated). It seems reasonable to believe that this difference was due to the much higher micelle-to-vesicle ratios in the original 90-min subphase and, perhaps, to the higher density of BS-rich micelles.

In concert with the observation that vesicles may in fact sediment rather than float during centrifugation, an analysis of a midduodenal sample (OH_2, 60 min) showed that lipid concentration in the unfractionated sample was 4.2 g/dL (Table III), but after centrifugation for 6×10^6 g·min, the resulting subphase had a lipid concentration of only 0.17 g/dL (3.7 mM), with a BS concentration at ≈cmc (1.8 mM, Table VI). The pellet, which was relatively large, had a composition (Table VII) that was more reminiscent of the emulsifying lipids (Table V) than of the subphase (Table VI). Since the subphase of this sample had a composition that plotted outside the micellar phase boundary (Figure 3) and the average particle $\bar{R}_h$ was 482 ± 7 Å (Table VIII), it seems likely that, because of a BS concentration approximating the cmc, the lipids in the pellet represented unsolubilized vesicles originating from the emulsion surface.

In a final set of experiments, we determined, by two-component QLS analysis (Figure 8), the proportion of lipids carried in mixed micelles compared with unilamellar vesicles and their

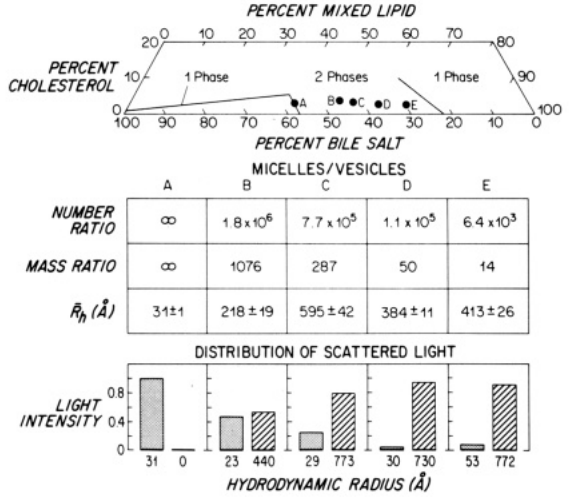

FIGURE 8: Two-component QLS analysis of duodenal subphase fractions. Top shows the relative lipid compositions that plot on the boundary of the micellar zone and progressively extend into the two-phase zone of the truncated model triangular coordinate system (Staggers et al., 1990). The middle panel displays number and mass ratios of micelles to vesicles as well as (mean) $\bar{R}_h$ values by QLS letter coded to the appropriate relative lipid composition. The bottom histogram shows the relative intensity of laser light scattered by coexisting micelles and vesicles as well as their individual R_h values (see text for details).

numerical ratio in five semiequilibrated, but unfractionated, subphases. The upper panel displays the relative lipid compositions plotted on appropriate truncated triangular coordinates for typical physiological conditions (Staggers et al., 1990): One sample plotted on the micellar phase boundary, while the remainder fell within the two-phase "physiological" region. The central panels depict the numerical and weight ratios of particles, as well as $\bar{R}_h$ values (angstroms) for each sample. The lower histograms show the proportion of light intensity scattered from micelles and vesicles and the individual R_h values of each particle population. Taken together, these show that, as the percent BS in the relative lipid composition (all with approximately the same mole percent Ch) decreased from the micellar phase boundary moving across the two-phase region, the number and mass ratio of micelles-to-vesicles decreased, the $\bar{R}_h$ values showed an abrupt increase from micellar to vesicle sizes, and the proportion of light scattered by micelles became progressively less. The individual R_h values show that the micellar composition was resolved in each sample and varied between 23 and 53 Å. These data also illustrate the important fact that nonmicellar particles, even at very low relative concentrations, have pronounced influences on mean $\bar{R}_h$ values. Hence, the two-phase sample (B) closest to the micellar phase boundary ($\bar{R}_h$ value of 218 Å) contained micelles of R_h = 23 Å and vesicles of R_h = 440 Å. However, upon computation of the w/w ratio in this subphase, the micelles accounted for all but one of every 1.8×10^6 particles present (Figure 8) and "carried" 99.9% of total lipids.

Discussion

Over 25 years ago, on the basis of gross examination and lipid analysis of ultracentrifuged human upper small intestinal contents following a lipid-rich meal, Hofmann and Borgström (1962, 1964) concluded that the physical–chemical states of all luminal lipids were distributed between an oil emulsion "phase" and a BS micellar phase. Shortly thereafter, an insoluble sedimentable phase of particulate matter was added to complete this description (Simmonds et al., 1967) but was thought to contain negligible lipid (Hofmann, 1968). Simmonds and colleagues (Simmonds et al., 1967) demonstrated, employing perfusion studies in healthy adult human beings, that absorption of dietary lipids without appreciable BS absorption took place in the upper jejunum from a BS mixed micellar solution containing primarily FA, 2-MG, and Ch. This model of the physical–chemical basis of fat digestion and absorption was widely accepted and has not been questioned until recently (Patton & Carey, 1979; Stafford & Carey, 1981; Carey, 1983a; Borgström, 1985). It has, however, been observed repeatedly that, following inactivation of pancreatic lipase by heating to 70 °C, the so-called micellar phase, when collected by prolonged (~24 h) ultracentrifugation (Hofmann & Borgström, 1962), was not invariably an isotropic, nonopalescent phase (Porter & Saunders, 1971; Poley et al., 1977). These earlier findings are compatible with the suggestion, made by Patton and Carey (Patton & Carey, 1979; Carey, 1983a) and later supported by Rigler and co-workers (Rigler et al., 1986), that the so-called micellar phase may actually be composed of a two-phase or multiphase system of liquid-crystalline particles of larger sizes suspended in a micellar solution. In fact, this was strongly suspected by Porter and Saunders (1971), who found that ultracentrifugal attempts to clarify the micellar phase invariably resulted in the establishment of a steep BS-plus-solubilized lipid gradient down the length of the centrifuge tubes with very low BS concentrations in the optically clear portions. In the microfiltration approach employed by Mansbach and colleagues (Mansbach et al., 1975), an approximate monomeric BS concentration was isolated through 15-Å filters. Reasoning that the retentates in these cells were concentrated micelles (after passage through a 2200-Å filter), they found that the FA-to-BS stoichiometry was 1.4 and the micellar sizes on monomeric BS-equilibrated Sepharose 4B columns were 23–35 Å. Further, using polarizing microscopy, these authors also noted smectic aggregates of liquid-crystalline lipid in some samples of "distal duodenal fluid".

In the present experiments and in our model systems with pure lipids (Staggers et al., 1990), we found direct in vitro support and an explanation for these diverse findings. When mixed BS, Ch, and other aqueous intestinal lipids (partially ionized FA, MG, and PL and traces of DG) were mixed to pattern the typical literature compositions of postprandial aqueous duodenal contents at pH 5.5–7.5 [e.g., Ricour and Rey (1970), Porter and Saunders (1971), Miettinen and Siurala (1971a), and Mansbach et al. (1975)], the relative lipid compositions plotted in a region containing two coexisting phases that were shown to be composed of mixed micelles and unilamellar vesicles. The typical molar ratio of BS-to-mixed lipids was approximately 1.4 at the boundary of the micellar phase (as plotted in Figure 4), in agreement with Mansbach and co-workers' (Mansbach et al., 1975) estimate for FA:BS alone, but varied with physiological conditions of pH, total lipid concentration, and FA:MG ratio (Staggers et al., 1990). In the present study, when the relative compositions of aqueous duodenal contents were plotted on triangular coordinates with appropriate variations in phase boundaries according to ex vivo conditions, most samples plotted within the two-phase region; however, several plotted within the micellar phase (Figures 3 and 4). Figure 9 displays plots of recalculated relative lipid compositions from published data on postprandial, so-called micellar, subphases from normal human subjects (Porter & Saunders, 1971; Zentler-Munro et al., 1984; Poley et al., 1977; Mansbach et al., 1975; Ricour & Rey, 1970; Miettinen & Siurala, 1971a; Badley et al., 1970; Schneider & Viteri, 1974a; Hardison & Rosenberg, 1967; Modai & Theodor, 1970;

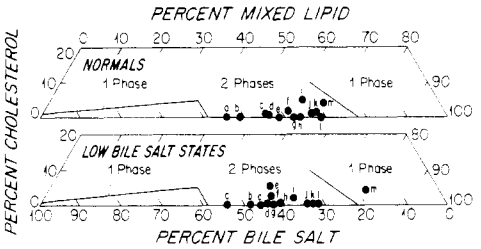

FIGURE 9: (Upper panel) Relative lipid compositions of subphases calculated from lipid analyses of aqueous duodenal contents from healthy humans in the literature. The truncated phase diagram is for model systems based upon typical intraluminal (duodenal) conditions (1 g/dL total lipid, FA:MG ratio 5:1, pH 6.5, 37 °C). Each data point represents the mean of from 3 to 30 analyses. Data points falling on the base axes indicate that subphase Ch concentrations were not reported. (a) Rautureau et al. (1981); (b) Badley et al. (1970); (c) Ricour and Rey (1970); (d) Poley et al. (1977); (e) Hardison and Rosenberg (1967); (f) Mansbach et al. (1975); (g) Roggin et al. (1972); (h) Porter & Saunders (1971); (i) Simmons and Bouchier (1972); (j) Modai and Theodor (1970); (k) Schneider and Viteri (1974a); (l) Zentler-Munro et al. (1984); (m) Miettinen and Siurala (1971a). It is apparent that all so-called micellar phases from these authors plot within the two-phase (micelles plus vesicles) zone of the phase diagram. (Lower panel) Relative lipid compositions of subphases calculated from lipid analyses of duodenal contents from human beings with low BS concentrations, with perturbed BS metabolism and/or enterohepatic cycling. Each data point represents mean values from a larger number of subjects. (a) Cystic fibrosis (Zentler-Munro et al., 1984); (b) ileectomy with BS supplement (Hardison & Rosenberg, 1967); (c) ileectomy (Van Deest et al., 1968); (d) viral hepatitis (Modai & Theodor, 1970); (e) celiac sprue (Miettinen & Siurala, 1971b); (f) icteric hepatic cirrhosis (Miettinen & Siurala, 1971b); (g) ileectomy (Hardison & Rosenberg, 1967); (h) chronic hepatic disease with steatorrhea (Badley et al., 1970); (i) Crohn's disease with or without ileectomy (Mansbach et al., 1980); (j) growth hormone deficiency (Poley et al., 1977); (k) cholecystectomy (Simmons & Bouchier, 1972); (l) protein caloric malnutrition (Schneider & Viteri, 1974b); (m) anicteric hepatic cirrhosis (Miettinen & Siurala, 1971b). These relative compositions show no appreciable differences in distribution compared with the normals in the upper panel. While the absolute concentrations of lipids in the subphases were less in the patients with low BS states, the physical-chemical states remain the same.

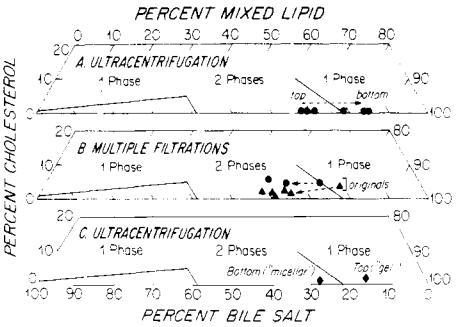

FIGURE 10: (A) Relative lipid compositions (Ch not measured) of subphase samples at sequential levels from top to bottom of the subphase following prolonged ultracentrifugation. The relative lipid compositions change in favor of more vesicles, and eventually a single phase of lamellar liquid crystals is produced at the bottom of the tubes, i.e., when BS concentrations fall below their cmc values (data of Porter and Saunders (1971)]. (B) Relative lipid compositions of original subphases after mild centrifugation and the final relative lipid compositions after multiple filtrations. A pure micellar phase was not obtained by these manipulations [data recalculated from results of Porter and Saunders (1971) (solid circles) and Mansbach et al. (1975) [solid triangles]. (C) Relative lipid compositions of subphases (n = 6) claimed to be micellar and a birefringent gel phase (n = 6) harvested at the interfaces between oil and subphase portions of ultracentrifuged postprandial upper small intestinal contents of healthy humans. By phase analysis, the micellar phase is a two-phase system and the gel phase is a lamellar liquid-crystalline phase [data replotted from results of Holt et al. (1986)].

Rauterau et al., 1981; Roggin et al., 1972; Simmons & Bouchier, 1972). As displayed here, all relative lipid compositions from normal subjects plotted within the two-phase physiological zone of the phase diagram where micelles and vesicles coexist. We carried out a similar plot (Figure 9) using literature values for aqueous duodenal contents aspirated from patients with various low intraluminal BS states (Badley et al., 1970; Modai & Theodor, 1970; Miettinen & Siurala, 1971b; Poley et al., 1977; Schneider & Viteri, 1974b; Zentler-Munro et al., 1984; Van Deest et al., 1968; Simmons & Bouchier, 1972; Mansbach et al., 1980; Hardison & Rosenberg, 1967). These also had a mixed lipid-to-BS ratio higher than 1.4 (micellar phase limit), and their relative lipid compositions, with one exception, plotted within the physiological two-phase zone (Figure 9); the exception fell not within the micellar phase but in the single-phase liquid-crystalline zone (Figure 9). Although, the very fast processes of lipid digestion and absorption can hardly ever represent fully developed equilibrium states, we showed in our model systems that the micellar phase boundaries are displaced to the right in the nonequilibrium state and at equilibrium with variations in physical-chemical conditions of physiological importance (Staggers et al., 1990). It is salutary, therefore, that only data points demarcated a in both plots in Figure 9 could have fallen within the micellar zone if such an expansion occurred. The present work, taken together with the published literature, clearly indicates that a pure micellar phase in aqueous duodenal contents is the exception, rather than the rule, under typical physiological conditions. It is, of course, quite likely that a pure micellar phase might be expected when dietary fat intake is very low or when the source of vesicles from lipolytic products is eliminated in the distal jejunum. The present work showed that in one subject (OH_2, 60 min) with a subphase BS concentration of 1.8 mM the pellet was greatly enriched in liquid-crystalline lipid—an observation not investigated previously in the cited low BS literature. Although Figure 9 establishes that *relative* lipid compositions of duodenal subphases do not differ between normals and patients with low BS states, the *absolute* lipid compositions are very different in that the dispersed aqueous lipid concentrations in the subphases of normals are invariably much higher.

Why investigators reported clear "micellar" phases of duodenal contents, which plot uniformly on our phase diagrams in a two-phase (micelle plus vesicle) region (Figure 9) where model mixtures were often found to be turbid (Staggers et al., 1990), bears scrutiny. First, some of these reported ex vivo systems were not, in fact, optically clear. For example, the 1000-Å filtrates of Porter and Saunders (1971) and Mansbach and co-workers (Mansbach et al., 1975) had notable optical densities, instead of zero, as would be expected for pure micellar solutions. As shown in Figure 10, all of the "final" (micellar) filtrates of these authors plotted well inside the physiological two-phase zone. However, the lipids in the bottom enrichment in the ultracentrifugation studies and the originals in the multiple filtration studies may well have been liquid crystalline, since pancreatic lipase was not inhibited (see literature data in Figure 10). Further, it must be appreciated that, while total lipid concentrations of isolated subphases rarely varied more than 0.25–1.5 g/dL, the micellar fraction by two-component QLS carried most of the lipid. Yet, at these low total lipid concentrations, even mixtures with relative compositions well within the two-phase region were apparently clear to the unaided eye. However, as we have shown in this work and in the preceding paper (Staggers et al., 1990), large vesicles can only be demonstrated to coexist in such native as well as model systems when their presence is monitored by a very sensitive technique such as QLS. Obviously, in the in-

vestigation of dilute aqueous lipid systems, optical clarity is not a sufficient criterion for defining a dilute micellar solution, whereas with higher total lipid concentration this may not be as serious a problem (Carey & Small, 1978; Staggers et al., 1990).

Methodological problems may also have contributed to the failure to detect a vesicle phase mixed with the micellar phase. Prolonged high-speed ultracentrifugation creates gradients of BS and other lipids within the centrifuge tube (Lee, 1972). This alters the BS-to-mixed lipid ratio in the aqueous subphase, as shown in the present work (Table VI) and in the plotted data of Porter and Saunders (1971) in Figure 10. Analysis of the relative lipid composition at each level within these reported gradients (Porter & Saunders, 1971) shows that all compositions plotted outside the micellar region (Figure 10). These results suggest that there was sequential exclusion of large liquid-crystalline structures so that a single optical analysis of the remaining highly dilute portions was insufficient to detect a vesicle phase. In the case of the work of Mansbach and co-workers (Mansbach et al., 1975), vesicles were excluded by filtration; however, the overall mixed lipid-to-BS ratios in their study were $\gg$1.4, appreciably greater than the FA:BS ratio, strongly suggesting that vesicles were present but overlooked in the micellar fractions. It is noteworthy that these authors obtained micellar sizes similar to ours (<40 Å) by gel chromatography; however, the V_0 shoulder of lipids in Figure 6 of their work (Mansbach et al., 1975) clearly indicates that gel filtration removed most of the coexisting vesicles in the void volume.

In equilibrated model systems (Staggers et al., 1990), tie-lines designating compositions of these coexisting phases suggested that both phases were saturated, i.e., BS micelles saturated with mixed lipids and mixed lipid vesicles saturated with BS. This is not in complete analogy to what we found in the present experiments, in that the micellar phase under nonequilibrium conditions of the upper small intestine was frequently unsaturated and in the process of becoming saturated, with lipid, as evidenced by the discordance between $\bar{R}_h$ values (Table VIII) and relative lipid compositions by phase analysis and by the spontaneous ability of subphases to dissolve their vesicles to form pure micellar phase systems. We did not attempt to characterize further by physical–chemical methods the various particles within the physiological two-phase region. The smaller vesicle sizes compared with model systems are indicative of the nonequilibrium nature of the intestinal environment, although other components, such as divalent ions, amphiphiles, proteins, or even lysolecithin, may have interfered with their growth. While it is possible that other product phases may be present, e.g., a hexagonal and/or a so-called L-2 (reversed micellar) phase, as suggested by Lindström and co-workers (Lindström et al., 1981) and Borgström (Borgström, 1985), our findings, based on multicomponent QLS, freeze-fracture electron microscopy, and, in some cases, partial ultracentrifugal separation of micelles from vesicles, are consistent only with mixed micelles and unilamellar vesicles. Our results are in agreement with recent in vitro and in vivo (killifish intestinal contents) freeze-fracture studies of Rigler and colleagues (Rigler et al., 1986).

Since our model experiments (Staggers et al., 1990) had revealed that phase boundaries shift with variations in total lipids, pH, and the FA:MG molar ratio and since incorrect compositions would profoundly influence deduction of the phase relations, it was necessary to use a rapid and nonperturbing method to inhibit lipolysis. Obviously the method using multiple chemical inhibitors, described in the present work, appears to have been rapid and highly effective (Table II) and less perturbing to the physical–chemical states (see Materials and Methods), compared to previous approaches such as heating to 70 °C (Hofmann & Borgström, 1964), multiple filtrations (Mansbach et al., 1975), and acidification, followed by neutralization (Zentler-Munro et al., 1984). For these reasons, since lipolysis continued to a marked degree in all earlier studies, the results of other authors were actually biased in favor of a higher proportion of vesicles to micelles (Figures 9 and 10) than in the present experiments (Figures 3 and 4).

A key question is the physical–chemical origin of the unilamellar vesicles. Our model experiments (Staggers et al., 1990) showed that metastable unilamellar vesicles of lipolytic products and BS formed spontaneously in vitro within the physiological two-phase region, suggesting that this would occur in vivo when lipolytic products were mixed with BS (possibly as part of the emulsifying coat) at the sites of production. Further, in our physical–chemical analysis of the interfaces by phase equilibria (Figure 2), as well as by polarizing microscopy, an excess of emulsifiers that included BS was present as lamellar liquid crystals (multilamellar vesicles or liposomes). It is of interest in this context that the average relative lipid composition of a verified lamellar liquid–crystalline (gel) phase (n = 6) from a postprandial study of Holt and colleagues (Holt et al., 1986) plotted within the one-phase liquid-crystalline zone of our phase diagram (Figure 10), and the so-called micellar phase of these authors fell within the two-phase (micelle plus vesicle) zone (Figure 10), consistent with our replotting of the data from other authors (Figure 9). In recent studies (Rigler et al., 1986), freeze-fracture electron microscopy has confirmed the budding of vesicles from multilamellar lipolytic products surrounding fat droplets in vitro and in rapidly frozen killifish intestinal lumen. In earlier studies, Lairon and co-workers (Lairon et al., 1980a,b) showed that the majority of biliary lipids in the rat rapidly adsorbed either by monomer diffusion or by bulk transport to coat the surface of the crude TG–rich emulsion particles with a mixed lipid monolayer. In an earlier study (Carey et al., 1983), Carey and co-workers suggested that pancreatic colipase-dependent lipase hydrolysis of TG and DG within the monolayer (Miller & Small, 1982) gave rise to a further interfacial accumulation of relatively polar lipids, chiefly 2-MG and partially ionized FA (acid soap). This was verified in the present study by analysis of the interfaces collected following centrifugation (Table V, Figure 2).

In analogy to what is known about the metabolism of TG-rich lipoproteins, it is tempting to speculate that, after the major part of emulsified TG has been hydrolyzed, a phase separation of core and surface lipids will occur (Miller & Small, 1983). Such phase separation was first observed by Patton and Carey (1979), who visualized lipolysis on microscope slides under conditions that were patterned after duodenal contents (Patton et al., 1985). Consequently, it is most likely that unilamellar vesicles are a primary *dispersed* product of fat digestion and that they are formed at the oil–H_2O interface, presumably via a multilamellar liquid-crystalline intermediate. If so, it was important that we observed vesicles to be heterogeneous both in size ($\bar{R}_h \simeq$ 200–600 Å) and composition (Figure 4). However, the observation that both micelles and vesicles failed to separate completely by ultracentrifugation was consistent with their similar buoyant densities. Generally, gradients were created in the centrifuge tubes upon second and third centrifugations; lower density vesicles were enriched at the top of the subphase and mixed, in part, with the interfacial particles. However, we also found

that vesicles could be enriched at the bottom of the subphase, indicating a higher density in some cases compared with micelles, as also shown by Porter and Saunders (1971) (Figure 10). One contributing factor might be the relative enrichment of bile pigments and divalent cations in larger uni- or multilamellar vesicles. Bilirubin has a density of ~ 1.3 g·cm^{-3} (Bonnett et al., 1978; Mugnoli et al., 1978), higher than that of most dietary lipids and their lipolytic products, hence the observed color gradient of partially oxidized bile pigments (yellow to green to olive/black) down the length of the centrifuged samples (Figure 1). In fact, a comparison of relative distribution of lipids in one subject with a low BS concentration (1.8 mM, OH_2 60-min total subphase, Table VI) within each separated fraction suggested that pelleted lipids originated directly from the emulsifiers on the emulsion's surface. It is indeed possible that both a unilamellar vesicle phase and a micellar subphase may be critically dependent upon a micellar BS concentration for both solubilization and multilamellar → unilamellar vesicle transformation [see Staggers et al. (1990)].

A further observation in the present work that supports the metastable nature of human upper intestinal contents was that unilamellar vesicles of the subphases were appreciably smaller than the sizes predicted by 5–7-day equilibration of the model systems (Figure 5). Further, these vesicles often spontaneously dissolved into mixed micelles with passage of time, strongly suggesting that they did not originate from supersaturated mixed micelles, in which case they would have been expected to grow in size (Staggers et al., 1990). This phenomenon was highlighted by QLS measurement of vesicle $\bar{R}_h$ values at early time points in samples of subphases whose relative lipid compositions plotted *within* the micellar phase (see Results). Rapid vesicle dissolution into mixed micelles was also in agreement with what we observed in model experiments, in that micellar samples with compositions similar to human bile could rapidly dissolve unilamellar vesicles (Staggers et al., 1990). However, a spontaneous conversion of vesicles to the average size of micelles was observed only in ex vivo samples with an initially high micelle-to-vesicle ratio and was slow; this suggested, on the basis of the model systems, that the micelles were near saturation with lipids. It must be appreciated, however, that, by design, the present studies were "frozen in time" by chemical inhibitors for ex vivo study; therefore, the continued production of lipolytic products at the oil–H_2O interface of the emulsion particles was essentially completely inhibited (Table II), as was the ex vivo depletion of micellar lipid by mucosal absorption.

Our results are compatible with the schematic model of the physical–chemical events in fat digestion, shown in Figure 11. Biliary lipids, which may be a two-phase micelle-plus-vesicle system in many adult human beings (Sömjen & Gilat, 1983; Pattinson, 1985), first mix with pancreatic lipase/colipase complex, and together adsorb to the crude DG and TG emulsion surfaces, entering from the stomach. The biliary lipids further stabilize the emulsion particles and reduce the emulsion's sizes (Carey et al., 1983). Because partially ionized FA and MG are also potent emulsifiers, and FA promote binding of the colipase-lipase complex to the emulsion surface (Borgström, 1980; Bernbäck et al., 1989), emulsification is further enhanced when lipolytic products are produced. The remaining biliary lipids, mainly PL, Ch, and BS, will remain as a coexisting micellar phase in aqueous duodenal contents and are continually replenished from the liver and gallbladder (Carey & Cahalane, 1988). During lipolysis, lipid products will locate mainly at the emulsion surface, presumably as multilamellar liquid-crystalline bilayers (Rigler et al., 1986;

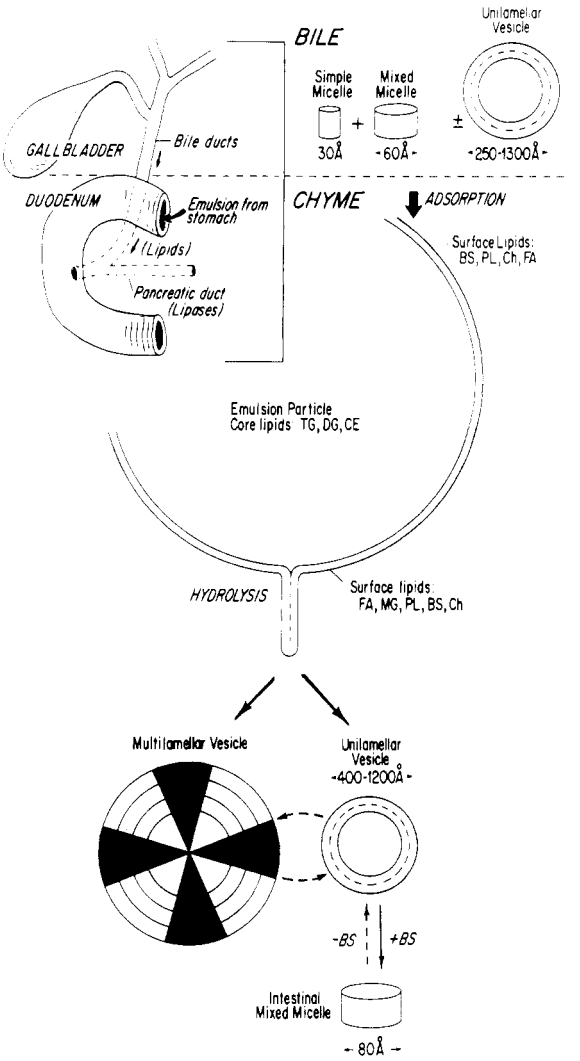

FIGURE 11: Proposed model for the sequential steps in fat digestion. Biliary lipids in various physical states (simple micelles, mixed micelles, and vesicles), together with pancreatic colipase-dependent lipase and colipase, adsorb to the surface of crude emulsion particles entering the duodenum from the stomach. The emulsions are stabilized by biliary lipids (Carey et al., 1983) and immediate lipolysis commences. This results in the rapid generation of lipolytic products in great excess on the emulsion's surface (Rigler et al., 1986). The shrinking of the oil core and building up of FA, PL, and MG (and BS) leads to enormous surface pressures—the core lipids dissociate from the surface lipids (possibly present as multilamellar layers, a lamellar liquid-crystalline phase; this work; Rigler et al., 1986; Holt et al., 1986) and then bud off as unilamellar vesicles. Following centrifugal separation of ex vivo samples, unilamellar vesicles and micelles coexist in the aqueous-rich portion of duodenal contents and are interconvertible generally in favor of micellar particles by unsaturated BS micelles. Lamellar liquid crystals and macroemulsion particles remain at the oil–subphase *interface* and, in many cases, lamellar liquid crystals are found in the precipitated pellet (not shown).

Holt et al., 1986). As the core of the emulsion droplet shrinks, parts of the surface coat pinch off as large liquid-crystalline structures. Provided sufficient bile salts are present, they will catalyze formation of small unilamellar vesicles from multilamellar liposomes in H_2O, and, in health, via the continued presence of bile, a two-phase system of vesicles and mixed micelles will form. Continually replenished from the biliary tree, micelles are generally unsaturated with PL, even when diluted in the duodenum, and will dissolve the swelling amphiphiles of vesicles. Provided dissolution is faster than mucosal absorption of lipid, micelles will become more and more saturated with products of lipolysis. It has been repeatedly observed that saturation of micelles with lipolytic products

provides the ideal thermodynamic environment for maximum rates of intestinal absorption of FA, MG, Ch, and other dietary and biliary lipids [reviewed in Thomson et al. (1989) and references cited therein]. The driving force down concentration gradients results in lipid product absorption, probably preferentially from micelles due to their larger number and, in the case of the intestinal lumen, unexpectedly small sizes and, thereby, their more rapid diffusive access to the mucosal surface. However, absorption could also take place from unilamellar and, perhaps, even multilamellar vesicles. Microscopically visible lamellar (smectic) liquid crystals were observed in interfaces and, also, in pellets in this study and clearly represent excess emulsifying lipid of the lipolytic products (Figure 2). Although Hofmann and Borgström (1962, 1964) made this prescient prediction, Mansbach and co-workers were the first to observe (Mansbach et al., 1975) a liquid-crystalline phase in human intestinal contents that layered in the ultracentrifuge tube between so-called micellar and oil phases. Only later was this proven to be a multilamellar (smectic) phase by Holt and colleagues (Holt et al., 1986). The abundance of multilamellar liquid crystals would explain the relatively unimpaired fat absorption seen with low or absent intraluminal BS concentrations, e.g., in patients with external bile fistula (Porter et al., 1971) or breast-fed preterm newborn infants (Signer et al., 1974; Hernell et al., 1988). However, the possible presence of unilamellar vesicles in the total absence of luminal BS remains to be proven, but it is likely that spontaneous vesiculation will occur in the presence of high dilution, physiological ionic strength, and multilayers of partially ionized FA (Hauser et al., 1986). Nevertheless, the broader significance of vesicle-mediated absorption involving other hydrophobic nutrients as well as pharmacological/environmental hydrophobic and hydrophilic xenobiotics is unknown. Recent evidence suggests that vesicles may serve as substrates for pancreatic nonspecific carboxyl ester hydrolase and, in the breast-fed infant, the BS-stimulated lipase of human milk (Hernell, 1985; Lindström, 1988).

ACKNOWLEDGMENTS

We are grateful to Dr. Patrick H. Griffin for help with the duodenal intubations, Dr. David E. Cohen for expert advice in quasielastic light scattering spectroscopy, Dr. James L. Madara for carrying out the freeze-fracture electron microscopy (Harvard Digestive Diseases Center, Morphology Core Laboratory), and Rebecca Ankener for expert word-processing, editorial, and bibliographic assistance. We are particularly indebted to Professor Bengt Borgström and an anonymous reviewer for their thorough and constructive criticisms of the manuscript.

Registry No. Ch, 57-88-5.

REFERENCES

Badley, B. W. D., Murphy, G. M., Bouchier, I. A. D., & Sherlock, S. (1970) *Gastroenterology 58*, 781–789.

Bartlett, G. R. (1959) *J. Biol. Chem. 234*, 3466–3468.

Bernbäck, S., Hernell, O., & Bläckberg, L. (1987) *Biochim. Biophys. Acta 922*, 206–213.

Bernbäck, S., Bläckberg, L., & Hernell, O. (1989) *Biochim. Biophys. Acta 1001*, 286–293.

Bitman, J., & Wood, D. L. (1981) *J. Liq. Chromatogr. 4*, 1023–1034.

Bitman, J., Wood, D. L., & Ruth, J. M. (1981) *J. Liq. Chromatogr. 4*, 1007–1021.

Bläckberg, L., Lombardo, D., Hernell, O., Guy, O., & Olivecrona, T. (1981) *FEBS Lett. 136*, 284–288.

Bonnett, R., Davies, J. E., Hursthouse, M. B., & Sheldrick, G. M. (1978) *Proc. R. Soc. London B202*, 249–268.

Borgström, B. (1977) *Int. Rev. Physiol 12*, 305–323.

Borgström, B. (1980) *Gastroenterology 78*, 954–962.

Borgström, B. (1985) *Scand. J. Gastroenterol. 20*, 389–394.

Borgström, B., & Erlanson-Albertsson, C. (1984) in *Lipases* (Borgström, B., & Brockman, H. L., Eds.) pp 152–183, Elsevier, Amsterdam.

Carey, M. C. (1983a) in *Phospholipids and Atherosclerosis* (Avogaro, P., Mancini, M., Ricci, G., & Paoletti, R., Eds.) pp 33–63, Raven Press, New York.

Carey, M. C. (1983b) in *Bile Acids in Gastroenterology* (Barbara, L., Dowling, R. H., Hofmann, A. F., & Roda, E., Eds.) pp 19–56, MTP Press, Lancaster, U.K.

Carey, M. C., & Small, D. M. (1978) *J. Clin. Invest. 61*, 998–1026.

Carey, M. C., & Cahalane, M. J. (1988) in *The Liver, Biology and Pathobiology* (Arias, I. M., Jacoby, W. B., Popper, H., Schachter, D., & Shafritz, D. A., Eds.) 2nd ed., pp 573–616, Raven Press, New York.

Carey, M. C., Small, D. M., & Bliss, C. M. (1983) *Annu. Rev. Physiol. 45*, 651–677.

Cohen, D. E. (1986) Ph.D. Dissertation, Harvard University, 8806072, pp 1–207, University Microfilms, Ann Arbor, MI, 1988.

DeHaas, G. H., Postema, N. M., Nieuwenhuizen, W., & Van Deenen, L. L. M. (1968) *Biochim. Biophys. Acta 159*, 103–117.

Folch, J., Lees, M., & Sloane-Stanley, G. H. (1957) *J. Biol. Chem. 226*, 497–509.

Gardner, C. W. (1980) *J. Biol. Chem. 255*, 5064–5068.

Gargouri, Y., Moreau, H., Piéroni, G., & Verger, R. (1988) *J. Biol. Chem. 263*, 2159–2162.

Hardison, W. G. M., & Rosenberg, I. H. (1967) *N. Engl. J. Med. 277*, 337–342.

Hauser, H., Gains, N., Eibl, H.-J., Müller, M., & Wehrli, E. (1986) *Biochemistry 25*, 2126–2134.

Hernell, O. (1985) *J. Pediatr. Gastroenterol. Nutr. 4*, 517–519.

Hernell, O., & Bläckberg, L. (1982) *Pediatr. Res. 16*, 882–885.

Hernell, O., Bläckberg, L., & Bernbäck, S. (1988) in *Perinatal Nutrition* (Lindblad, B. S., Ed.) pp 259–272, Academic Press, New York.

Hofmann, A. F. (1960) *Biochem. J. 89*, 57–68.

Hofmann, A. F. (1968) in *Medium Chain Triglycerides* (Senior, J. R., Ed.) pp 9–19, Saunders, Philadelphia.

Hofmann, A. F., & Borgström, B. (1962) *Fed. Proc. 21*, 43–50.

Hofmann, A. F., & Borgström, B. (1964) *J. Clin. Invest. 43*, 247–257.

Hofmann, A. F., & Mekhjian, H. S. (1973) in *The Bile Acids* (Nair, P. P., & Kritchevsky, D., Eds.) Vol. 2, pp 103–152, Plenum Press, New York.

Holt, P. R., Fairchild, B. M., & Weiss, J. (1986) *Lipids 21*, 444–446.

Lairon, D., Charbonnier-Augeire, M., Nalbone, G., Leonardi, J., Hauton, J. C., Pieroni, G., Ferrato, F., & Verger, R. (1980a) *Biochim. Biophys. Acta 618*, 106–118.

Lairon, D., Nalbone, G., Lafont, H., Leonardi, J., Vigne, J.-L., Chabert, C., Hauton, J. C., & Verger, R. (1980b) *Biochim. Biophys. Acta 618*, 119–128.

Lee, K. Y. (1972) *J. Lipid Res. 13*, 745–749.

Lindström, M. (1988) Doctoral thesis, University of Lund, Sweden.

Lindström, M., Ljusberg-Wahren, H., Larssen, K., & Borgström, B. (1981) *Lipids 16*, 749–754.
Lombardo, D. (1982) *Biochim. Biophys. Acta 700*, 67–74.
Lombardo, D., & Guy, O. (1980) *Biochim. Biophys. Acta 611*, 147–155.
Lowry, O. H., Rosebrough, N. H., Farr, A. L., & Randall, R. J. (1951) *J. Biol. Chem. 193*, 265–275.
Madara, J. L. (1983) *J. Cell Biol. 97*, 125–136.
Mansbach, C. M., Cohen, R. S., & Leff, P. B. (1975) *J. Clin. Invest. 56*, 781–791.
Mansbach, C. M., Newton, D., & Stevens, R. D. (1980) *Dig. Dis. Sci. 25*, 353–362.
Maylie, M. F., Charles, M., & Desnuelle, P. (1972) *Biochim. Biophys. Acta 276*, 162–175.
Mazer, N. A., Carey, M. C., Kwasnick, R. F., & Benedek, G. B. (1979) *Biochemistry 18*, 3064–3075.
Miettinen, T. A., & Siurala, M. (1971a) *Z. Klin. Chem. Klin. Biochem. 9*, 47–52.
Miettinen, T. A., & Siurala, M. (1971b) *Scand. J. Gastroenterol. 6*, 527–535.
Miller, K. W., & Small, D. M. (1982) *J. Colloid Interface Sci. 89*, 466–478.
Miller, K. W., & Small, D. M. (1983) *J. Biol. Chem. 258*, 13772–13784.
Modai, M., & Theodor, E. (1970) *Gastroenterology 58*, 379–387.
Moreau, H., Gargouri, Y., Bernadal, A., Pieroni, G., & Verger, R. (1988) *Rev. Fr. Corps Gras 35*, 169–176.
Mugnoli, A., Manitto, P., & Monti, D. (1978) *Nature 273*, 568–569.
Pattinson, N. R. (1985) *FEBS Lett. 181*, 339–342.
Patton, J. S. (1981) in *Physiology of the Gastrointestinal Tract* (Johnson, L. R., Ed.) pp 1123–1146, Raven Press, New York.
Patton, J. S., & Carey, M. C. (1979) *Science 104*, 145–148.
Patton, J. S., Vetter, R. D., Hamosh, M., Lindström, M., Borgström, B., & Carey, M. C. (1985) *Food Microstruct. 4*, 29–41.
Poley, J. R., Smith, J. D., Thompson, J. B., & Seely, J. R. (1977) *Pediatr. Res. 12*, 1186–1191.
Porter, H. P., & Saunders, D. R. (1971) *Gastroenterology 60*, 997–1007.
Porter, H. P., Saunders, D. R., Tytgat, G., Brunser, O., & Rubin, C. E. (1971) *Gastroenterology 60*, 1008–1019.
Rautureau, M., Bisalli, A., & Rambaud, J.-C. (1981) *Gastroenterol. Clin. Biol. 5*, 417–425.
Ricour, C., & Rey, J. (1970) *Rev. Eur. Etud. Clin. Biol. 15*, 287–293.
Rigler, M. W., Honkanen, R. E., & Patton, J. S. (1986) *J. Lipid Res. 27*, 836–857.
Roggin, G. M., Iber, F. I., & Linscheer, W. G. (1972) *Gut 13*, 107–111.
Schneider, R. E., & Viteri, F. E. (1974a) *Am. J. Clin. Nutr. 27*, 777–787.
Schneider, R. E., & Viteri, F. E. (1974b) *Am. J. Clin. Nutr. 27*, 788–796.
Signer, E., Murphy, G. M., Edkins, S., & Anderson, C. M. (1974) *Arch. Dis. Child. 79*, 174–180.
Simmonds, W. J., Hofmann, A. F., & Theodor, E. (1967) *J. Clin. Invest. 46*, 874–890.
Simmons, F., & Bouchier, I. A. D. (1972) *S. Afr. Med. J. 46*, 2089–2092.
Small, D. M. (1971) in *The Bile Acids* (Nair, P. P., & Kritchevsky, D., Eds.) Vol. 1, pp 249–356, Plenum Press, New York.
Small, D. M. (1986) *The Physical Chemistry of Lipids*, pp 1–672, Plenum Press, New York.
Sömjen, G. J., & Gilat, T. (1983) *FEBS Lett. 156*, 265–268.
Stafford, R. J., & Carey, M. C. (1981) *Clin. Res. 29*, 511A (Abstract).
Stafford, R. J., Donovan, J. M., Benedek, G. B., & Carey, M. C. (1981) *Gastroenterology 80*, 12 (Abstract).
Staggers, J. E., Frost, S. C., & Wells, M. A. (1982) *J. Lipid Res. 23*, 1143–1150.
Staggers, J. E., Hernell, O., Stafford, R. J., & Carey, M. C. (1990) *Biochemistry* (preceding paper in this issue).
Thomson, A. B. R., & Dietschy, J. M. (1981) in *Physiology of the Gastrointestinal Tract* (Johnson, L. R., Ed.) pp 1147–1220, Raven Press, New York.
Thomson, A. B. R., Keelan, M., Garg, M. L., & Clandinin, M. T. (1989) *Can. J. Physiol. Pharmacol. 67*, 179–191.
Turley, S. D., & Dietschy, J. M. (1978) *J. Lipid Res. 19*, 924–928.
Van Deest, B. W., Fordtran, J. S., Morawski, S. G., & Wilson, J. D. (1968) *J. Clin. Invest. 47*, 1314–1324.
Verger, R. (1984) in *Lipases* (Borgström, B., & Brockman, H. L., Eds.) pp 121–150, Elsevier, Amsterdam.
Verheij, H. M., Volwerk, J. J., Jansen, E. H. J. M., Puyk, W. C., Dijkstra, B. W., Drentin, J., & DeHaas, G. H. (1980) *J. Am. Chem. Soc. 102*, 743–750.
Zentler-Munro, P. L., Fine, D. R., Fitzpatrick, W. J. F., & Northfield, T. C. (1984) *Gut 25*, 491–499.